

The Genomic Landscape of Intrinsic and Acquired Resistance to Cyclin-Dependent Kinase 4/6 Inhibitors in Patients with Hormone Receptor–Positive Metastatic Breast Cancer



Seth A. Wander^{1,2,3,4}, Ofir Cohen^{1,2,4}, Xueqian Gong⁵, Gabriela N. Johnson^{1,2,4}, Jorge E. Buendia-Buendia^{1,2,4}, Maxwell R. Lloyd^{1,2}, Dewey Kim^{1,2,4}, Flora Luo^{1,2,3,4}, Pingping Mao^{1,2,3,4}, Karla Helvie^{1,2}, Kailey J. Kowalski^{1,2,4}, Utthara Nayar^{1,2,3,4}, Adrienne G. Waks^{1,2,3,4}, Stephen H. Parsons⁵, Ricardo Martinez⁵, Lacey M. Litchfield⁵, Xiang S. Ye⁵, Chunping Yu⁵, Valerie M. Jansen⁵, John R. Stille⁵, Patricia S. Smith⁵, Gerard J. Oakley⁵, Quincy S. Chu⁶, Gerald Batist⁷, Melissa E. Hughes^{1,2}, Jill D. Kremer⁵, Levi A. Garraway^{1,2,3,4,5}, Eric P. Winer^{2,3}, Sara M. Tolaney^{2,3}, Nancy U. Lin^{2,3}, Sean G. Buchanan⁵, and Nikhil Wagle^{1,2,3,4}

ABSTRACT

Mechanisms driving resistance to cyclin-dependent kinase 4/6 inhibitors (CDK4/6i) in hormone receptor-positive (HR⁺) breast cancer have not been clearly defined. Whole-exome sequencing of 59 tumors with CDK4/6i exposure revealed multiple candidate resistance mechanisms including *RB1* loss, activating alterations in *AKT1*, *RAS*, *AURKA*, *CCNE2*, *ERBB2*, and *FGFR2*, and loss of estrogen receptor expression. *In vitro* experiments confirmed that these alterations conferred CDK4/6i resistance. Cancer cells cultured to resistance with CDK4/6i also acquired *RB1*, *KRAS*, *AURKA*, or *CCNE2* alterations, which conferred sensitivity to *AURKA*, ERK, or CHEK1 inhibition. Three of these activating alterations—in *AKT1*, *RAS*, and *AURKA*—have not, to our knowledge, been previously demonstrated as mechanisms of resistance to CDK4/6i in breast cancer preclinically or in patient samples. Together, these eight mechanisms were present in 66% of resistant tumors profiled and may define therapeutic opportunities in patients.

SIGNIFICANCE: We identified eight distinct mechanisms of resistance to CDK4/6i present in 66% of resistant tumors profiled. Most of these have a therapeutic strategy to overcome or prevent resistance in these tumors. Taken together, these findings have critical implications related to the potential utility of precision-based approaches to overcome resistance in many patients with HR⁺ metastatic breast cancer.

INTRODUCTION

The cyclin-dependent kinase 4/6 inhibitors (CDK4/6i) have entered widespread use in both the first- and subsequent-line setting for patients with hormone receptor-positive (HR⁺), human epidermal growth factor receptor 2 negative (HER2⁻) metastatic breast cancer (MBC; refs. 1, 2). Their application has resulted in significant improvements in progression-free survival (PFS) and overall survival (OS) for treatment-naïve and previously treated patients in combination with anti-estrogens (3–9). Abemaciclib has shown efficacy as a single agent in endocrine-refractory disease and has been approved for use as monotherapy in pretreated patients with HR⁺/HER2⁻ MBC (10). Despite these advances, HR⁺/HER2⁻ MBC remains a significant cause of morbidity and mortality. Many patients demonstrate *de novo* (or intrinsic) resistance to these agents, and, in those who respond, acquired resistance and disease progression are unfortunately inevitable.

We have limited insight into the molecular pathways governing resistance to CDK4/6i. Early development of these

compounds indicated preferential efficacy in luminal/RB-positive cell lines (11). Loss of RB expression has been identified in cellular models cultured to resistance in CDK4/6i and rare *RB1* alterations have been identified in tumor samples and circulating tumor DNA (ctDNA) from patients with CDK4/6i exposure (12–14).

The PI3K pathway has also been implicated in mediating CDK4/6i resistance, with multiple effectors downstream of PI3K, including PTEN and PDK1, identified both *in vitro* and in patient samples, though the role of PI3K itself in resistance remains less clear (15–18).

Preclinical studies have also implicated overexpression of CDK6 and cyclin E2 (*CCNE2*) in mediating resistance (19, 20), whereas increased expression of cyclin E1 (*CCNE1*) was associated with inferior response to palbociclib in tumor samples (21).

Prior work from our laboratory has implicated alterations in *ERBB2* and *FGFR2* in mediating resistance to CDK4/6i *in vitro* and in patients (22, 23).

Here we explore the genomic landscape of resistance to CDK4/6i via whole-exome sequencing (WES) of metastatic tumor biopsies. We demonstrate that the landscape of resistance to CDK4/6i is heterogeneous, with multiple potential mediators including biallelic *RB1* disruption and activation of *AKT1*, *RAS*, *ERBB2*, *FGFR2*, *AURKA*, and *CCNE2*. Modification of HR⁺ breast cancer cells, via CRISPR-mediated knock-out or lentiviral overexpression, corroborates the candidate mechanisms of resistance identified by tumor sequencing. Cells cultured to resistance in the presence of CDK4/6i demonstrate concordant alterations in *RB1*, *AURKA*, and *CCNE2* expression along with *RAS*/ERK activation and demonstrate enhanced sensitivity to novel targeted therapies. In one patient with HR⁺/HER2⁻ MBC that progressed on first-line CDK4/6i, *AURKA* inhibition provoked prolonged disease control in a phase I clinical trial. These results shed new light on the diverse landscape of genomic alterations that drive resistance to CDK4/6i in HR⁺/HER2⁻ MBC and provide

¹Center for Cancer Precision Medicine, Dana-Farber Cancer Institute, Boston, Massachusetts. ²Department of Medical Oncology, Dana-Farber Cancer Institute, Boston, Massachusetts. ³Harvard Medical School, Boston, Massachusetts. ⁴Broad Institute of MIT and Harvard, Cambridge, Massachusetts. ⁵Eli Lilly and Co., Indianapolis, Indiana. ⁶Cross Cancer Institute, Alberta, Canada. ⁷Segal Cancer Centre, Jewish General Hospital, McGill University, Montreal, Canada.

Note: Supplementary data for this article are available at Cancer Discovery Online (<http://cancerdiscovery.aacrjournals.org/>).

S.A. Wander, O. Cohen, and X. Gong contributed equally to this article.

Corresponding Author: Nikhil Wagle, Dana-Farber Cancer Institute, 450 Brookline Avenue, Dana 820A, Boston, MA 02215. Phone: 617-596-3957; Fax: 617-582-7880; E-mail: nikhil_wagle@dfci.harvard.edu

Cancer Discov 2020;10:1174–93

doi: 10.1158/2159-8290.CD-19-1390

©2020 American Association for Cancer Research.

preclinical and translational rationale for novel strategies to circumvent and overcome resistance.

RESULTS

The Genomic Landscape of Intrinsic and Acquired CDK4/6i Resistance

We identified patients with HR⁺/HER2⁻ MBC who were treated with CDK4/6i with or without an antiestrogen and provided metastatic tumor biopsies as part of an institutional review board (IRB)-approved tissue collection protocol (24). We classified samples as reflecting sensitivity, intrinsic resistance, or acquired resistance (Fig. 1A). Sensitive biopsies were defined as baseline samples obtained within 120 days prior to, or up to a maximum of 31 days after, CDK4/6i initiation in a patient with subsequent clinical benefit (defined as radiographic response or stable disease >6 months). Biopsies reflecting intrinsic resistance were obtained within 120 days prior to or any time after CDK4/6i initiation in patients without evidence of clinical benefit (defined as progression on the first interval restaging study or stable disease <6 months). Biopsies reflecting acquired resistance were obtained from patients who had experienced clinical benefit with CDK4/6i and had an available biopsy specimen within 31 days prior to progression or at any time thereafter.

WES was successfully performed on 59 biopsies from 58 patients within the appropriate exposure window to be assigned a phenotype and with sufficient clinical data to define response (Supplementary Table S1). This included 18 sensitive biopsies, 28 intrinsic resistance biopsies, and 13 acquired resistance biopsies. The majority of patients (55, 94.8%) received standard combinations of an aromatase inhibitor or fulvestrant and a CDK4/6 inhibitor. Forty-nine patients (84.5%) received a palbociclib-based regimen, including 28 patients (48.3%) with an aromatase inhibitor and 20 patients (34.5%) with fulvestrant. The mean duration of therapy was 316 days (range, 43–1,052). Patients received an average of 1.5 lines of therapy in the metastatic setting (range, 0–7) and 30 patients (51.7%) had prior antiestrogen exposure in the metastatic setting. Additional clinical parameters are described in Supplementary Table S2.

WES of all 59 samples demonstrated a number of genomic alterations in genes implicated in HR⁺ breast cancer (*ESR1*, *PIK3CA*, *CCND1*, *FGFR1*, *TP53*) as well as additional cancer genes and putative resistance mediators (*RBI*, *ERBB2*, *FGFR2*, *AKT1*, *KRAS*, *HRAS*, *NRAS*, among others; Fig. 1B; Supplementary Table S3). Many of these alterations were enriched

in resistant samples and not present or relatively infrequent in sensitive samples, suggesting they might be contributing to resistance (Fig. 1B; Supplementary Fig. S1; Supplementary Table S4). In addition to these genomic differences, 3 patients with resistant tumor biopsies demonstrated loss of estrogen receptor (ER) expression in the metastatic drug-resistant tumor (measured by IHC); all patients were known to be ER⁺ at the time of metastatic diagnosis.

Although isolated amplification events were identified in a variety of cancer genes (Supplementary Table S4), amplification events in *AURKA* occurred more frequently in resistant samples as compared with sensitive samples (0 in sensitive, 26.8% in resistant; 0.0081, Welch test; Fig. 1C). Although only moderate-magnitude *AURKA* amplifications were seen among the resistant tumors, in The Cancer Genome Atlas (TCGA) study, even low *AURKA* amplification in primary HR⁺ breast cancer samples resulted in a statistically significant increase in gene expression (Supplementary Fig. S2), suggesting that the degree of *AURKA* amplification observed in the CDK4/6i-resistant cohort is likely to have a meaningful effect on gene expression and protein level.

On the basis of prior preclinical studies and known biology, we hypothesized that at least the following eight specific categories of alterations that were enriched in the resistant tumors were contributing to CDK4/6i resistance: biallelic disruption of *RBI*, activating mutation and/or amplification of *AKT1*, activating mutations in *KRAS/HRAS/NRAS*, activating mutations and/or amplification of *FGFR2*, activating mutations in *ERBB2*, amplification of *CCNE2*, amplification of *AURKA*, and loss of ER. We note that there is significant enrichment in *TP53* mutations among resistant specimens; however, additional preclinical and translational insights (described below) suggested that, despite this clear enrichment, *TP53* itself was not sufficient to drive the resistant phenotype. Beyond these, there are additional alterations that are enriched among resistant specimens, but we did not pursue these in further detail for this study.

In total, 27 of 41 resistant biopsies (65.9%) had genomic alterations in at least one of these 8 potential resistance mechanisms, as compared with 3 of the 18 sensitive biopsies (17%; Fig. 1D; Supplementary Table S5). Consistent with prior reports, biallelic disruption in *RBI* was exclusively present in resistant samples and occurred in a minority of resistant biopsies ($n = 4/41$, 9.8%). We identified diverse mechanisms of biallelic *RBI* disruption across the affected patients. In all examples, a single copy loss was noted in

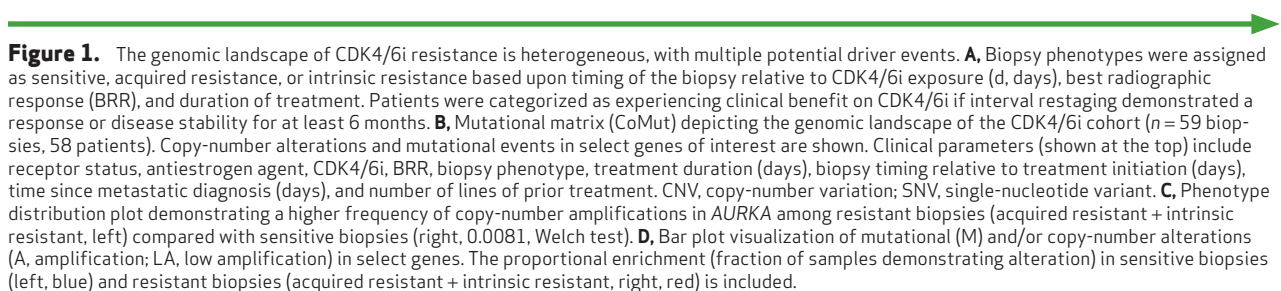
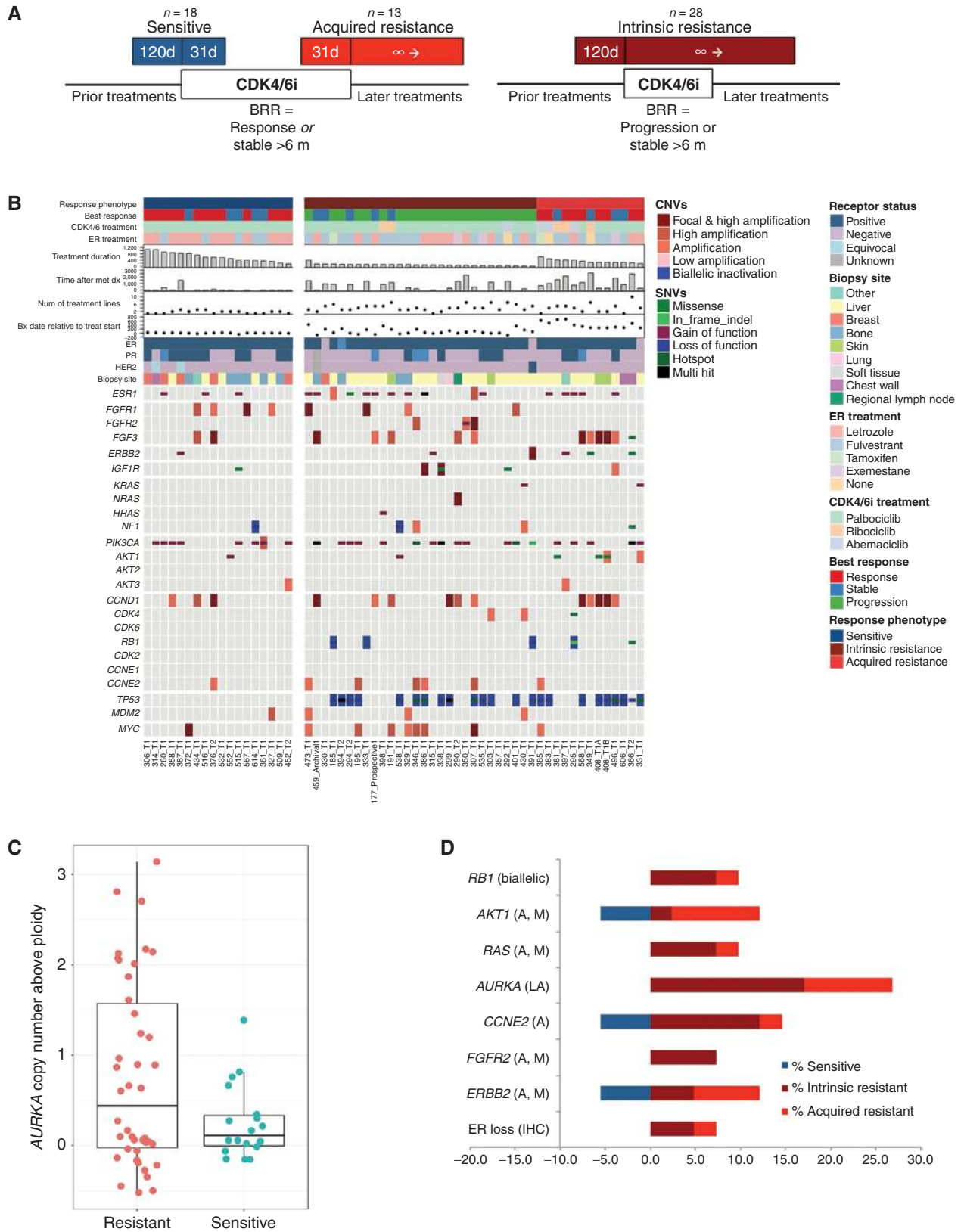


Figure 1. The genomic landscape of CDK4/6i resistance is heterogeneous, with multiple potential driver events. **A**, Biopsy phenotypes were assigned as sensitive, acquired resistance, or intrinsic resistance based upon timing of the biopsy relative to CDK4/6i exposure (d, days), best radiographic response (BRR), and duration of treatment. Patients were categorized as experiencing clinical benefit on CDK4/6i if interval restaging demonstrated a response or disease stability for at least 6 months. **B**, Mutational matrix (CoMut) depicting the genomic landscape of the CDK4/6i cohort ($n = 59$ biopsies, 58 patients). Copy-number alterations and mutational events in select genes of interest are shown. Clinical parameters (shown at the top) include receptor status, antiestrogen agent, CDK4/6i, BRR, biopsy phenotype, treatment duration (days), biopsy timing relative to treatment initiation (days), time since metastatic diagnosis (days), and number of lines of prior treatment. CNV, copy-number variation; SNV, single-nucleotide variant. **C**, Phenotype distribution plot demonstrating a higher frequency of copy-number amplifications in *AURKA* among resistant biopsies (acquired resistant + intrinsic resistant, left) compared with sensitive biopsies (right, 0.0081, Welch test). **D**, Bar plot visualization of mutational (M) and/or copy-number alterations (A, amplification; LA, low amplification) in select genes. The proportional enrichment (fraction of samples demonstrating alteration) in sensitive biopsies (left, blue) and resistant biopsies (acquired resistant + intrinsic resistant, right, red) is included.



Downloaded from <http://aacrjournals.org/cancerdiscovery/article-pdf/10/8/1174/1814347/1174.pdf> by guest on 27 August 2022

the presence of a point mutation, splice-site alteration, or frameshift event in the second allele.

AKT1 alterations were identified in five resistant biopsies ($n = 5/41$, 12.2%), including both mutations and amplifications. A single sensitive biopsy also demonstrated an activating *AKT1* alteration ($n = 1/18$, 5.6%).

Diverse RAS-pathway activating events were observed in four CDK4/6i-resistant cases ($n = 4/41$, 9.8%) including canonical activating mutations in *KRAS*^{G12D}, a pathogenic mutation in *KRAS*^{Q61L} (25), a mutation in *HRAS*^{K117N} (26, 27), and high focal amplification in *NRAS* (Fig. 1B). There were no instances of RAS-altered tumors with a sensitive phenotype.

Amplification events in *AURKA* were identified in 11 resistant biopsies ($n = 11/41$, 26.8%), including examples of both intrinsic and acquired resistance ($n = 7$ and $n = 4$, respectively). There were no sensitive biopsies with *AURKA* amplification.

There were six instances ($n = 6/41$, 14.6%) of *CCNE2* amplification identified across the resistant cohort (Fig. 1B). A single sensitive biopsy with a *CCNE2* alteration was identified ($n = 1/18$, 5.6%).

FGFR2 alterations were noted in three resistant biopsies (all with intrinsic resistance; $n = 3/41$, 7.3%), whereas mutations or amplification of *ERBB2* was noted in five resistant biopsies ($n = 5/41$, 12.2%). Of note, two of the *ERBB2* alterations identified (L377M and P1074L) were variants of uncertain significance, and the role of these specific mutations in provoking resistance to CDK4/6i has not been demonstrated. A single sensitive biopsy with an *ERBB2* alteration was also identified ($n = 1/18$, 5.6%).

With respect to ER expression, three resistant biopsy samples exposed to CDK4/6i and an antiestrogen demonstrated loss of ER expression via IHC ($n = 3/41$, 7.3%); there were no patients with ER loss among the sensitive tumor samples (Fig. 1B; Supplementary Table S5). These results are consistent with preclinical work demonstrating that CDK4/6i was predominantly effective in HR⁺ luminal cell lines whereas HR⁻ basal cell lines demonstrated frequent intrinsic resistance (11).

Enrichment in *ESR1* mutations was appreciated among resistant tumors ($n = 14/41$, 34.1%; Supplementary Table S4) compared with sensitive tumors ($n = 3/18$, 16.7%). *ESR1* mutations among sensitive tumors occurred exclusively in patients receiving fulvestrant and were not found in patients who achieved clinical benefit with CDK4/6i and an aromatase inhibitor, as would be expected (Supplementary Fig. S1A and S1B; ref. 28). These results support the notion that *ESR1* mutations are frequently acquired during the development

of endocrine resistance, while also suggesting that they are not sufficient to drive simultaneous resistance to CDK4/6i.

Among the 41 resistant biopsy samples, 15 (36.6%) had exactly one of these eight potential mechanisms of resistance and 12 (29.3%) had two or more of these resistance drivers concurrently. These include, for example, concurrent *ERBB2* and *AURKA* alterations in samples 349_T1 and 366_T2 as well as concurrent ER loss and alterations in *AKT1* and *KRAS* in sample 331_T1 (Supplementary Fig. S3).

Enrichment of a variety of additional genes was noted when comparing resistant and sensitive biopsy samples. Significant enrichment in *TP53* alterations was demonstrated across the resistant cohort (sensitive $n = 0/18$, 0%; resistant $n = 24/41$, 58.5%). Examples of *IGF1R* amplification (sensitive $n = 1/18$, 5.6%; resistant $n = 4/41$, 9.8%), *NF1* alteration (sensitive $n = 1/18$, 5.6%; resistant $n = 4/41$, 9.8%), and *MYC* amplification (sensitive $n = 1/18$, 5.6%; resistant $n = 8/41$, 19.5%) were also demonstrated across the cohort. *CCND1* alterations were also more common in resistant biopsies ($n = 11/41$, 26.8%) when compared with sensitive biopsies ($n = 3/18$, 16.7%).

Notably, mutational events in *PIK3CA* occurred frequently in both sensitive ($n = 8/18$, 44.4%) and resistant ($n = 18/41$, 43.9%) specimens, suggesting that *PIK3CA* is unlikely to be a marker of resistance. Copy-number gains in *FGFR1* were also noted among both sensitive ($n = 4/18$, 22.2%) and resistant ($n = 4/41$, 9.8%) biopsies.

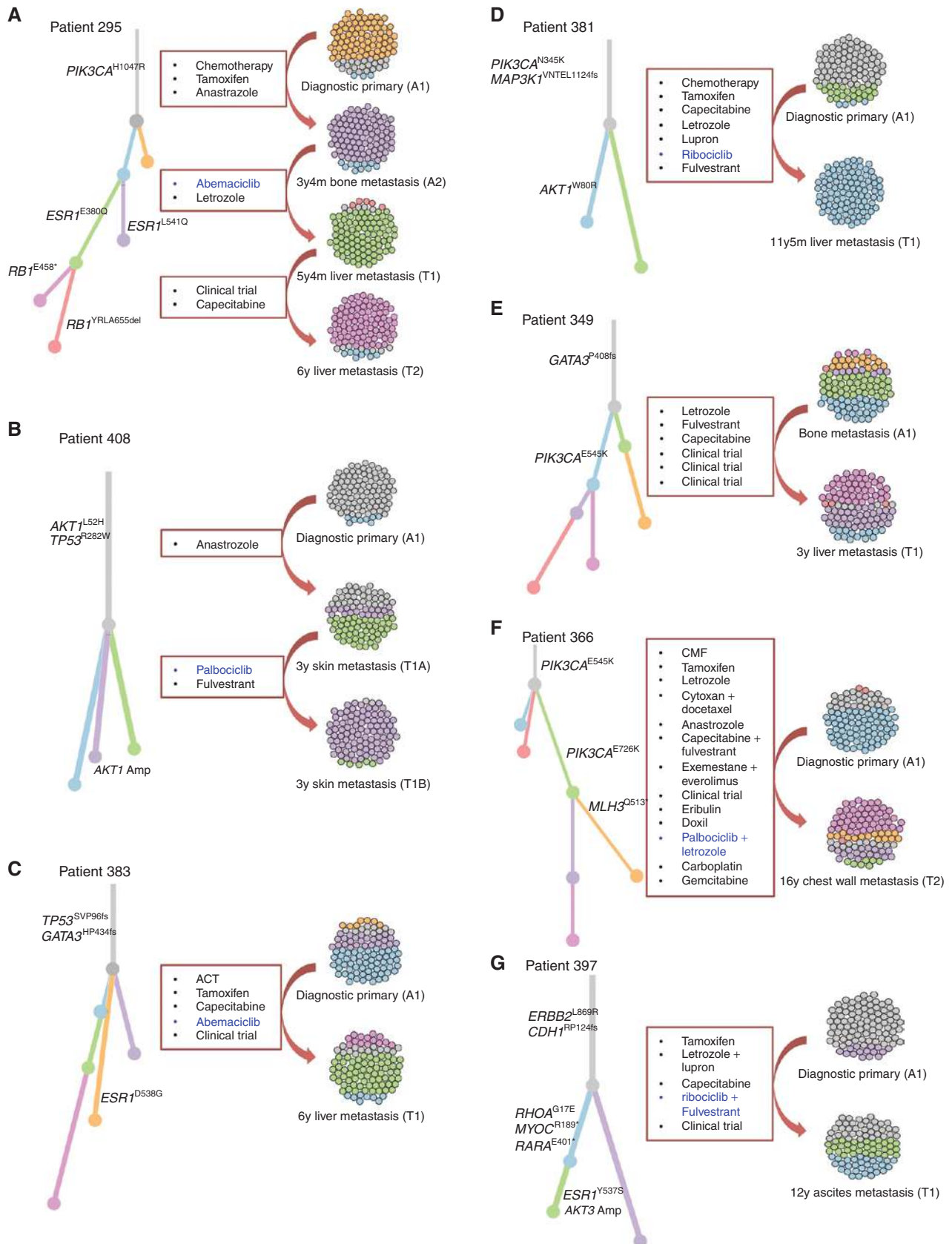
Systematic differences in the relative proportion of potential resistance alterations were not apparent when comparing the intrinsic and acquired resistance subgroups, although the power of this analysis is limited by sample size (Fig. 1D; Supplementary Table S4).

Evolutionary Dynamics in Acquired CDK4/6i Resistance

Matched pre- and post-treatment samples were available from 7 patients who experienced acquired resistance to CDK4/6i. We compared the WES from the paired pretreatment and post-treatment samples and performed an evolutionary analysis to evaluate clonal structure and dynamics, including changes in mutations and copy number. We established the evolutionary classification of each mutation to distinguish events that were acquired or enriched in clones that are dominant in the postprogression tumor, as compared with the pretreatment counterpart (Fig. 2; Supplementary Table S6).

Potential drivers of resistance that were observed in evolutionary acquired clones included a biallelic *RB1* disruption (Fig. 2A), an *AKT1* amplification (Fig. 2B), and an *AKT1* activating mutation (Fig. 2D).

Figure 2. Acquired resistance to CDK4/6i in patients with pretreatment and postprogression biopsies demonstrates convergent evolution of biallelic *RB1* disruption and evolved *AKT1* activation. Phylogenetic analysis depicting the evolutionary history for 7 patients with acquired alterations, with clonal evolutionary dynamics demonstrating: (A) acquired polyclonal *ESR1* mutations after aromatase inhibition, followed by convergent evolution of *RB1* inactivation, with different *RB1*-inactivating mutations acquired in two parallel sibling clones; (B) acquired *AKT1* amplification; (C) no notable candidate for acquired mechanism of resistance; (D) acquired *AKT1* (W80R) mutation; (E) no notable candidate for acquired mechanism of resistance; (F) acquired inactivation of DNA mismatch repair protein (MLH3); and (G) acquired activating *ESR1* mutation (Y537S) and amplification in *AKT3*. Branch colors in the phylogenetic trees match colors in the cell clouds for each patient, such that each color represents a subclone within the tumor cell population. Branch lengths are proportional to the number of mutations private to that subclone, and the prevalence of each subclone is represented by relative proportion of colored cells in the cell clouds. The treatment regimen containing the CDK4/6 inhibitor is highlighted in blue. CMF, cyclophosphamide, methotrexate, and fluorouracil.



Downloaded from <http://aacrjournals.org/cancerdiscovery/article-pdf/10/8/1174/1814347/1174.pdf> by guest on 27 August 2022

In the patient with biallelic *RB1* disruption and an available matched pair for exome analysis, the pretreatment specimen demonstrated a single copy deletion in *RB1*. Two separate postprogression biopsy samples demonstrated unique alterations in the second copy of *RB1*, suggesting convergent evolution toward a common mechanism of resistance within the same tumor ecosystem (Fig. 2A).

Genomic diversity was also observed in various mechanisms of AKT activation. In 2 patients with matched pre/post-treatment exome pairs, we observed acquisition of a pathogenic *AKT1* point mutation (*W80R*; refs. 29–31; Fig. 2D) and acquisition of an *AKT1* copy-number amplification in the background of an *AKT1* variant of uncertain significance (*L52H*), which was present at baseline (Fig. 2B). Taken together, these cases suggest that cancer clones with activated AKT by either pathogenic mutation or high copy number can confer selective advantage under CDK4/6i treatment.

In four of these pairs, the mechanism of acquired resistance remains unclear (Fig. 2C, E–G). We did not identify any instances of acquired *AURKA* overexpression, RAS activation, or *CCNE2* amplification, although the analysis was limited by number of available matched pairs.

Clinical Case Histories of Patients with CDK4/6i Resistance

Figure 3 illustrates the clinical details of selected patients with intrinsic and acquired resistance to CDK4/6i and putative driver alterations. These include four instances of biallelic *RB1* disruption (Fig. 3A), three patients with *AKT1* activation (Fig. 3B), three with RAS activation (Fig. 3C), and three with high *CCNE2* amplification (Fig. 3D).

Supplementary Figure S4 illustrates the three sensitive biopsy counterexamples: a single instance of *AKT1* activation (Supplementary Fig. S4A), a patient with low-level *CCNE2* amplification (Supplementary Fig. S4B), and a single *ERBB2* alteration (Supplementary Fig. S4C), all with clinical benefit on CDK4/6i.

Given the prominent (or exclusive) enrichment of *RB1* disruption, *AKT1* activation, *RAS* mutation, *AURKA* amplification, and *CCNE2* amplification within samples demonstrating resistance to CDK4/6i, we opted to pursue additional molecular validation of these targets. Prior work from our group and others implicating FGFR pathway and *ERBB2* activation in CDK4/6i resistance has been reported elsewhere (22, 23, 32). Although additional potential alterations of interest were noted in genes including in *IGF1R*, *NF1*, and *MYC* (among others), in this study we opted to focus on functional validation of the subset of resistance mediators highlighted above.

Candidate Alterations Provoke Resistance to CDK4/6i and Antiestrogens In Vitro

T47D and MCF7 HR⁺/HER2⁻ breast cancer cells were utilized to explore whether these five genetic alterations confer resistance to CDK4/6i *in vitro*. *AKT1*, *KRAS*^{G12D}, *AURKA*, and *CCNE2* were overexpressed via lentiviral transduction; *RB1* was inactivated via CRISPR-mediated knockout (Fig. 4A; Supplementary Fig. S5A). The impact of these alterations on susceptibility to CDK4/6i inhibitors was examined. Consistent with sequencing results, all alterations were sufficient to cause resistance to either palbociclib or abemaciclib in T47D cells (Fig. 4B–F). Corresponding IC₅₀ estimates for each dose-response curve are provided (Supplementary Table S7). Similar results were obtained in MCF7 cells (Supplementary Fig. S5B–S5F), although *AURKA* did not provoke resistance to CDK4/6i in this cell line, suggesting that context dependence may explain differences between cell lines, as with biopsies.

Of note, MCF7 (*TP53* wild-type) and T47D (*TP53* mutant) both demonstrate baseline sensitivity to CDK4/6i *in vitro*, suggesting that *TP53* itself may not be sufficient to drive resistance. To further validate this assumption, *TP53* expression was prevented in MCF7 via CRISPR-mediated knockout (Supplementary Fig. S6A). Loss of *TP53* did not provoke any resistance to escalating doses of palbociclib or abemaciclib *in vitro* (Supplementary Fig. S6B), further supporting the notion that loss of *TP53* function is not sufficient to drive CDK4/6i resistance.

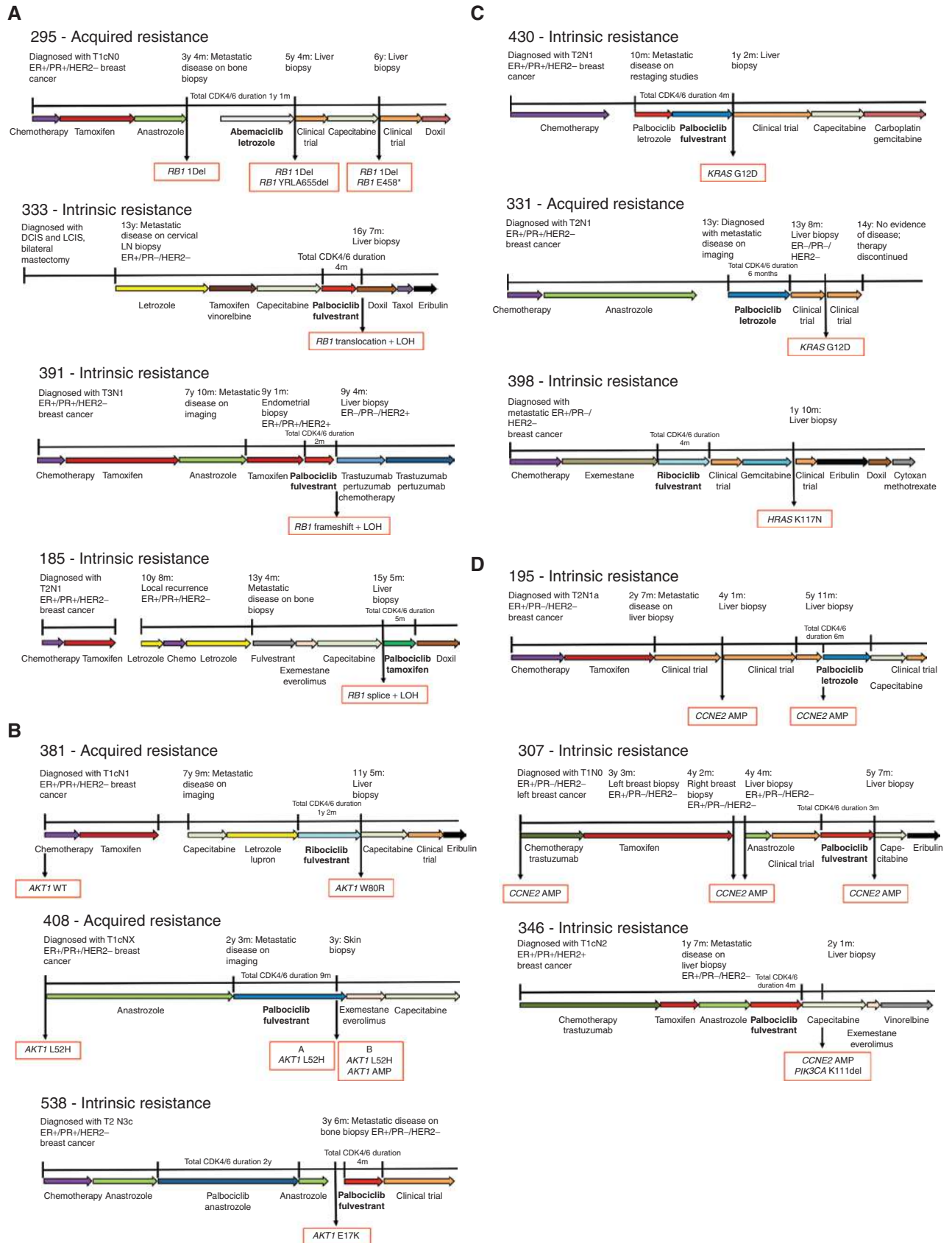
Given that most patients in the clinic are treated with a combination of CDK4/6i and an antiestrogen, we also explored sensitivity to fulvestrant (Supplementary Fig. S7A–S7E). Cells lacking *RB1* were only minimally resistant to fulvestrant monotherapy in both T47D and MCF7. Both *AKT1* and *CCNE2* overexpression conveyed resistance to fulvestrant in T47D and MCF7. Both *KRAS*^{G12D} and *AURKA* overexpression provoked significant resistance to fulvestrant in T47D cells but not in MCF7 cells.

Taken together, these results underscore the biological complexity related to the emergence of clinical resistance to these drug combinations both *in vitro* and in patients. They suggest that the resistance mechanisms identified in patient samples may provoke differential resistance to the CDK4/6- and estrogen-based components of the treatment regimen, and that these effects may depend upon additional cell-specific features.

Resistance Mediators Arise Independently during Culture to Resistance and Define New Dependencies In Vitro

Given the results identified via exogenous manipulation of the mediators described above, we sought to explore resistance

Figure 3. Clinical vignettes for candidate resistance drivers in representative patients (*RB1*, *AKT1*, *RAS*, and *CCNE2*). Clinical vignettes including treatment sequence, timing of metastatic progression, and available biopsies with key genomic findings are provided for the following: **A**, 4 patients with biallelic alterations in *RB1*, including a patient with multiple biopsies and convergent evolution toward *RB1* disruption (top; phylogenetic analysis for this patient is provided in Fig. 2A). **B**, Three patients with acquired alterations in *AKT1* following progression on CDK4/6i. In the first (top), a new mutation in *AKT1*^{W80R} was identified. In the second (middle), a baseline alteration (*AKT1*^{L52H}) was identified at the time of diagnosis; at the time of progression on CDK4/6i, two biopsies were obtained—both demonstrating the baseline *AKT1*^{L52H} mutation, one also demonstrating an acquired amplification of the wild-type *AKT1* protein (phylogenetic analyses for these patients are provided in Fig. 2B and D). **C**, Three patients with resistance to CDK4/6i and RAS family alterations (including two instances of *KRAS*^{G12D} and one instance of *HRAS* mutation). **D**, Three patients with intrinsic resistance to CDK4/6i and amplification events in *CCNE2*.



Downloaded from <http://aacrjournals.org/cancerdiscovery/article-pdf/10/8/1174/1814347/1174.pdf> by guest on 27 August 2022

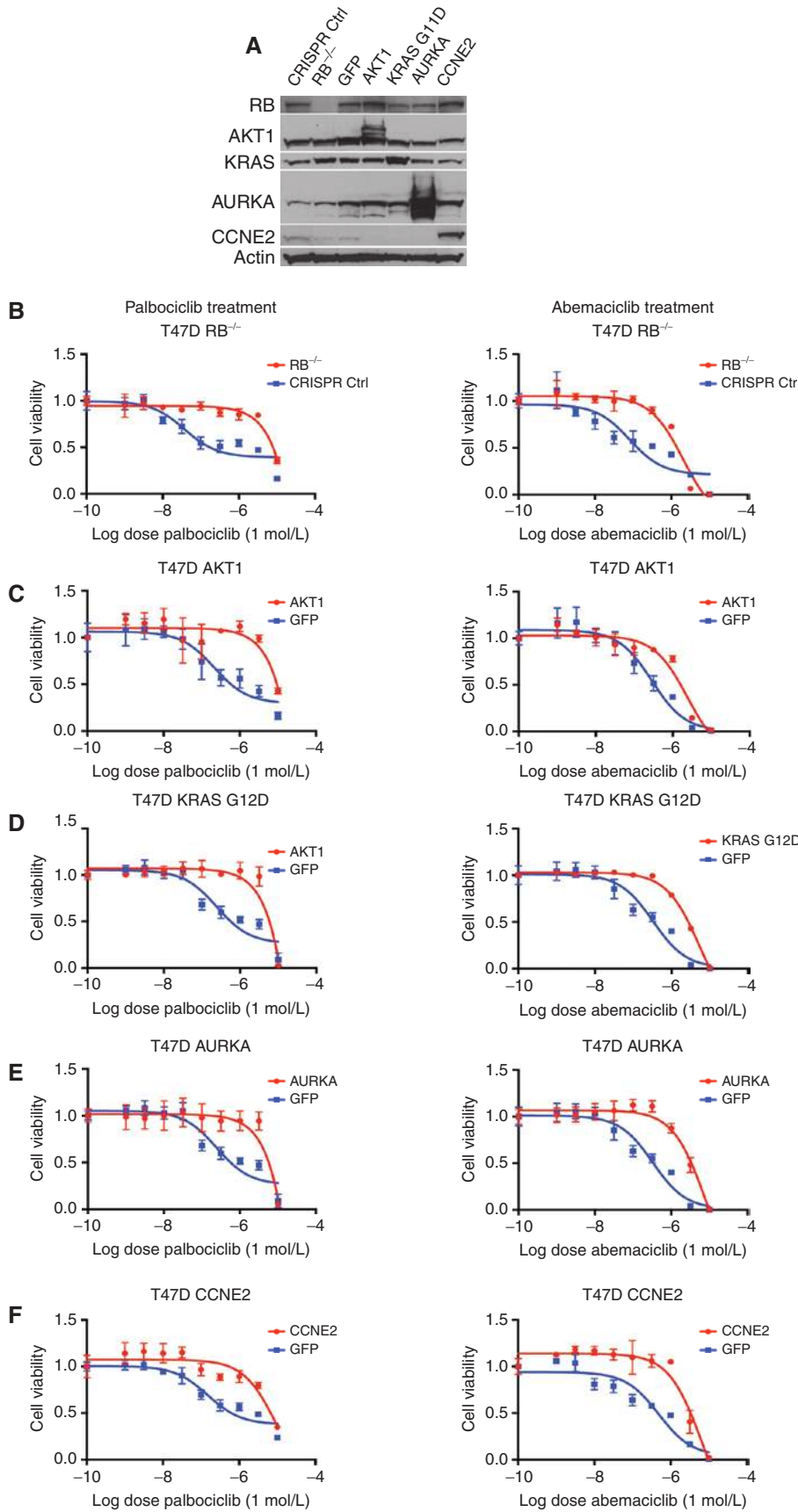


Figure 4. Candidate genomic alterations provoke CDK4/6i resistance *in vitro*. **A**, T47D cells were modified via CRISPR-mediated downregulation (RB1) or lentiviral overexpression (AKT1, KRAS^{G12D}, AURKA, CCNE2) to interrogate potential resistance mediators identified in patient biopsy samples. Western blotting with the indicated antibodies is included. **B-F**, Modified T47D cells were exposed to escalating doses of CDK4/6i (palbociclib, left; abemaciclib, right) and viability was estimated via CellTiter-Glo assay. Control (CRISPR nontargeting guide or GFP) cells are plotted along with the resistance driver of interest [RB1 (**B**), AKT1 (**C**), KRAS^{G12D} (**D**), AURKA (**E**), CCNE2 (**F**)]. Parental and variant cell lines are normalized to vehicle control, and viability is plotted as a function of increasing CDK4/6i (graphed as triplicate average ± SD). All variants provoke CDK4/6i resistance (to both palbociclib and abemaciclib) *in vitro* in T47D cells. Corresponding IC₅₀ values are included in Supplementary Table S7.

Downloaded from <http://aacrjournals.org/cancerdiscovery/article-pdf/10/8/1174/1814347/1174.pdf> by guest on 27 August 2022

to CDK4/6i via orthogonal platforms in the laboratory. The HR⁺ cell lines T47D, MCF7, and MDA-MB-361 were cultured to resistance in the presence of increasing doses of palbociclib or abemaciclib. To examine whether the putative drivers identified in patients were also responsible for resistance under selection *in vitro*, we characterized the resistant derivatives for levels of retinoblastoma protein, aurora kinase, cyclin E2, and for activated effectors of KRAS (Fig. 5A).

Many of the putative resistance drivers identified via patient sequencing emerged spontaneously under selective pressure *in vitro*. 361-AR-1 (a derivative of MDA-MB-361 cells cultured to resistance in abemaciclib) was found to have an oncogenic KRAS^{G12V} mutation (data not shown) and demonstrated increased ERK activation (Fig. 5A). Proteomic analysis showed activation of multiple MAPK pathway components, including ERK, MEK, and RSK (Supplementary Fig. S8). T47D-AR-1 (a derivative of T47D cells cultured to resistance in abemaciclib) demonstrated decreased RB1 along with increased AURKA and pERK (Fig. 5A). 361-PR-1 (a derivative of MDA-MB-361 cells cultured to resistance in palbociclib) demonstrated increased AURKA and CCNE2 protein levels (Fig. 5A). Finally, MCF7-PR-1 (a derivative of MCF7 cells cultured to resistance in palbociclib) demonstrated increased expression of CCNE2 (Fig. 5A). All derivative cell lines were confirmed to be resistant to abemaciclib compared with their parental counterparts (Fig. 5B).

Therapeutic approaches are suggested by alterations identified in patient tumor specimens and cell lines cultured to resistance (Fig. 5C). 361-AR-1 cells demonstrated increased KRAS/ERK activity and enhanced sensitivity to LY3214996, a selective ERK inhibitor. Both AURKA-amplified and RB1-low cells (T47D-AR-1 and 361-PR-1) were highly sensitive to LY3295668, a selective AURKA inhibitor that has previously been reported to show synthetic lethality with RB1 loss (33).

In lung cancer cells expressing high levels of AURKA, sensitivity to AURKA inhibition was dependent on multiple proteins which play a role in the mitotic checkpoint complex (MCC) to efficiently facilitate spindle apparatus assembly and mitotic exit (33). We explored the expression of two MCC effectors (BUB1R and MAD2), both of which were increased in 361-PR-1 cells, suggesting that the MCC protein complex may play an important role in mediating AURKA-dependent cell-cycle progression (and sensitivity to AURKA inhibition) in multiple tumor types (Supplementary Fig. S9).

Finally, cancers with high cyclin E and CDK2 activation have been reported to be dependent on CHEK1 (34). CCNE2-amplified cells (MCF7-PR-1) demonstrated increased sensitivity to prexasertib, a CHEK1 inhibitor. MCF7-PR-1 cells also demonstrated increased apoptotic activity with escalating doses of prexasertib when compared with the parental cells (Supplementary Fig. S10A and S10B). Corresponding IC₅₀ values for CDK4/6i and targeted agent treatment for these cell lines are included in Supplementary Table S8.

When compared with tumor sequencing results from patients with progression on CDK4/6i, the spontaneous emergence of corresponding alterations *in vitro* lends further support to the roles RB1 loss, RAS activation, CCNE2 overexpression, and AURKA overexpression may play in mediating resistance. That these alterations arose in parallel

in different cancer cell lines (akin to different patients) also supports the earlier observation that cellular context may dictate which alterations arise under selective pressure via CDK4/6i. These results suggest that, in the presence of specific driver alterations in resistant tumor cells, unique dependencies may emerge that could inform novel therapeutic strategies.

AURKA Inhibition Resulted in Prolonged Clinical Benefit in a Patient with HR⁺/HER2⁻, RB1⁺ MBC Following Progression on CDK4/6i-Based Therapy

LY3295668, the same AURKA-specific inhibitor utilized *in vitro* to demonstrate a new dependence on AURKA in MDA-MB-361 and T47D cells cultured to resistance in CDK4/6i (Fig. 5B and C), has entered early-stage clinical trials (NCT03092934).

As a proof-of-concept example, we provide the case history of a patient with locally advanced HR⁺/HER2⁻ breast cancer treated on the trial. She had chemotherapy and adjuvant tamoxifen prior to metastatic recurrence; at that time, she was treated with first-line palbociclib and letrozole (Fig. 6A). After prolonged clinical benefit on this regimen (>3 years), she progressed and enrolled on study with LY3295668. Her first restaging studies demonstrated disease stability, which persisted for approximately 11 months (Fig. 6A, top). IHC staining of her pretreatment liver biopsy following progression on CDK4/6i demonstrated high levels of the proliferative marker Ki-67 and high RB1 protein expression (Fig. 6A, bottom). These findings suggest that the mechanism of sensitivity to AURKA inhibition was not due to downregulation of RB1 protein expression. Sufficient additional biopsy material was not available for further sequencing or IHC-based analysis at the time of this writing. Sensitivity to AURKA inhibition in this patient could be due to alternative resistance mechanisms, such as AURKA amplification, though we cannot rule out other mechanisms of RB1 inactivation not detectable by IHC.

DISCUSSION

CDK4/6 inhibitors, in combination with an antiestrogen, have emerged as the standard of care for HR⁺/HER2⁻ MBC. Despite their widespread use, we have limited understanding of the mechanisms governing resistance, and deciphering that landscape constitutes a critically important unmet need. To our knowledge, we provide the first analysis based upon WES of sensitive and resistant tumor tissues in a diverse cohort of patients who received CDK4/6i. This effort confirmed previous reports implicating rare events affecting RB1 while also revealing novel mediators of resistance including AKT1, RAS family oncogenes, AURKA, CCNE2, and ER loss. Prior work from our group and others identified mutational events in ERBB2 (23) and the FGFR pathway (22, 32, 35) in driving resistance.

Although a variety of potential mediators appear to contribute to the heterogeneous landscape of resistance, several broad categories of resistance drivers have emerged, including regulators of the cell cycle and a variety of oncogenic signal transducers, providing rationales for new therapeutic strategies in the clinic (Fig. 6B).

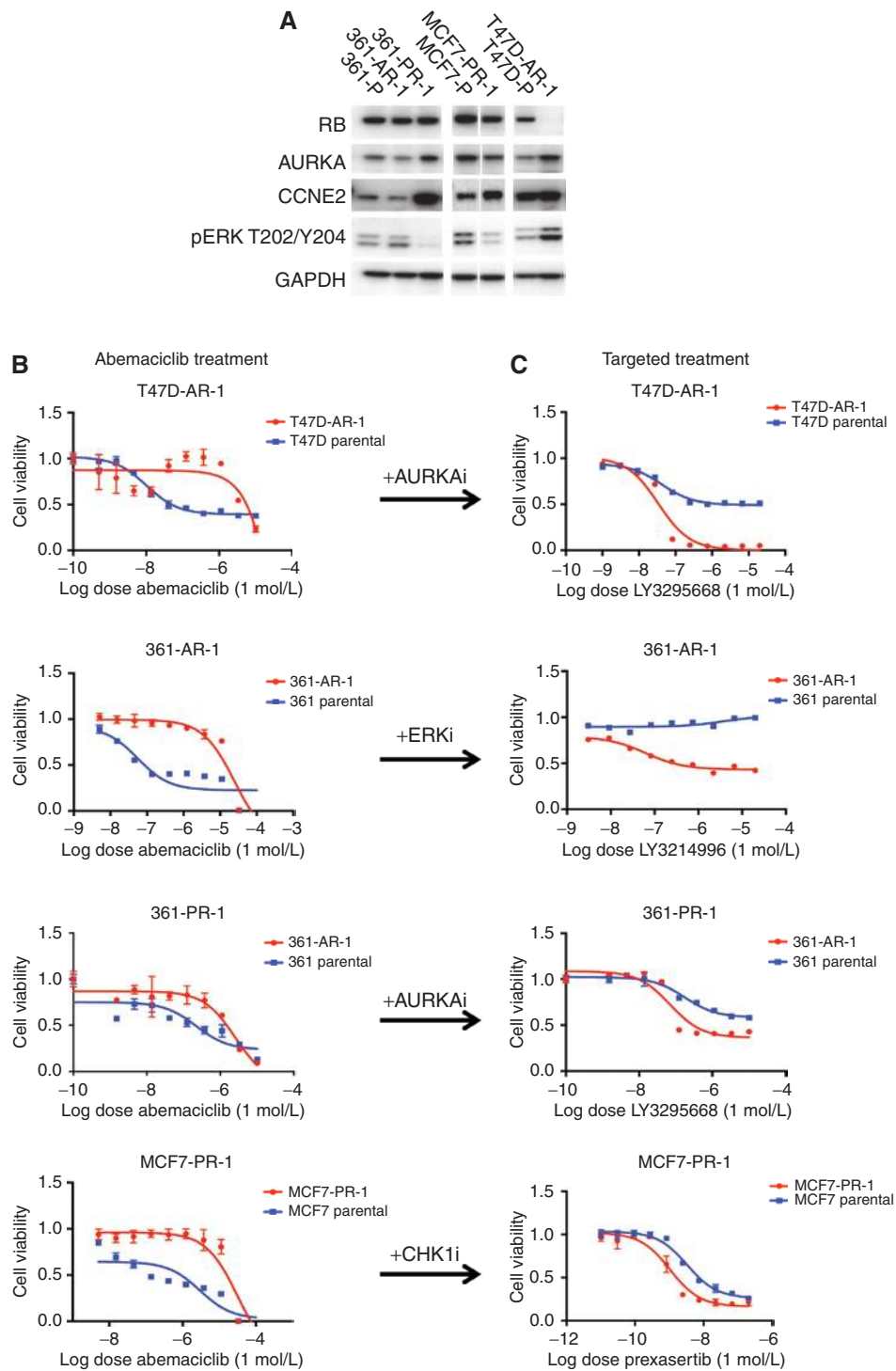


Figure 5. Candidate mutations emerge in cell lines cultured under CDK4/6i selective pressure and define new therapeutic dependencies *in vitro*. **A**, Breast cancer cell lines (T47D, MCF7, MDA-MB-361) were cultured long-term to resistance in the presence of CDK4/6i (palbociclib, abemaciclib). The resulting cell lines that emerged were subjected to Western blotting for putative mediators of drug resistance (RB1, AKT1, KRAS/ERK, AURKA, and CCNE2). **B** and **C**, T47D cells cultured to resistance in the presence of abemaciclib demonstrated low levels of RB1 expression (T47D-AR1) and increased sensitivity to the AURKA inhibitor LY3295668. MDA-MB-361 cells cultured to resistance in the presence of abemaciclib demonstrated high levels of ERK activation (361-AR1) and increased sensitivity to the ERK inhibitor LY3214996. MDA-MB-361 cells cultured to resistance in the presence of palbociclib demonstrated high levels of AURKA (361-PR1) and increased sensitivity to the AURKA inhibitor LY3295668. MCF7 cells cultured to resistance in the presence of palbociclib demonstrated increased levels of CCNE2 (MCF7-PR1) and increased sensitivity to the CHEK1 inhibitor prexasertib.

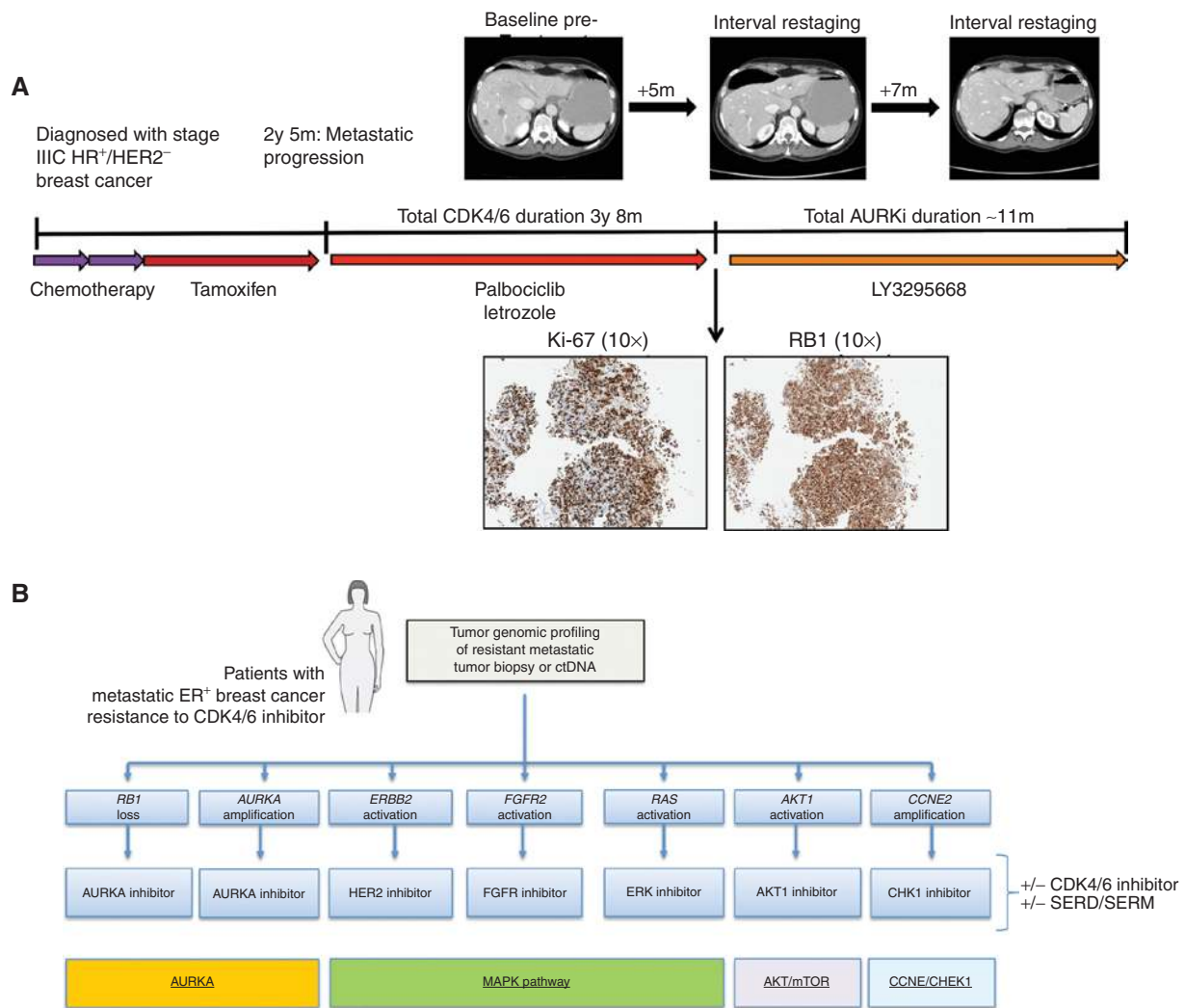


Figure 6. A novel AURKA inhibitor demonstrates therapeutic efficacy in a patient with metastatic HR⁺ breast cancer after progression on CDK4/6i. **A**, A patient with locally advanced HR⁺/HER2⁻ breast cancer developed metastatic recurrence on adjuvant tamoxifen. She received CDK4/6i and letrozole in the first-line setting with prolonged clinical benefit (>3 years). At progression, she was placed on trial with the AURKA inhibitor LY3295668; she subsequently experienced prolonged disease control for approximately 11 months. Baseline staging studies following progression on CDK4/6i in the patient described are included (top); she had osseous metastatic disease and visceral disease limited to the foci noted in the liver. Two interval restaging studies (top) demonstrate disease stability/mild response. Liver biopsy obtained at the time of progression on CDK4/6i and prior to LY3295668 demonstrated high Ki-67 and high RB1 protein expression via IHC (IHC, 10x; bottom). **B**, Schematic diagram demonstrating the potential utility of next-generation sequencing following progression on CDK4/6i; actionable alterations in *RB1*, *ERBB2*, *FGFR2*, *AKT1*, *RAS*, *AURKA*, and *CCNE2* could dictate informed selection of targeted therapies as indicated.

Cell Cycle-Regulatory Proteins as Key CDK4/6i Resistance Effectors

Several cell cycle-regulatory proteins have been implicated in driving CDK4/6i resistance, including RB1, CDK6, CCNE1, CCNE2, and AURKA. Despite its central role downstream of CDK4/6, alterations in *RB1* were observed only in a small fraction of patients who developed resistance to CDK4/6i. This is consistent with prior studies. One small case series demonstrated acquired alterations in *RB1* at the time of progression via ctDNA sequencing in 3 patients with exposure to CDK4/6i (13). ctDNA analysis from 195 patients treated on the PALOMA-3 study with fulvestrant and palbociclib also demonstrated rare *RB1* alterations (~5%), uniquely enriched

in the palbociclib-containing arm (14). Finally, a recent study in which pretreatment biopsies were subjected to targeted sequencing showed alterations in *RB1* in approximately 3%, associated with significantly impaired PFS on CDK4/6i (36). Our data supports the notion that *RB1* alterations occur in a small fraction of CDK4/6i-resistant patients (4/41, ~9.8%) and we provide new insight into diverse mechanisms of biallelic disruption. In a single patient with multiple pre- and post-treatment biopsies, two distinct mechanisms of biallelic inactivation were identified in separate postprogression biopsies, demonstrating convergent evolution under selective pressure for tumors with single copy loss *in vivo*. These findings were supported by culture to resistance experiments,

in which multiple cell lines downregulated RB1 expression under selective pressure. Although the rate of genomic *RB1* disruption in tumor samples appears to be low following progression, additional nongenomic events may be missed by targeted or exome-based sequencing (such as methylation, mutations in regulatory regions, or post-translational modification). These possibilities warrant additional study.

Several prior studies highlight CDK6 alteration as a mechanism of resistance to CDK4/6 inhibitors (19). Although clinical studies have not identified any examples of *CDK6* alterations in resistant samples, a recent study that performed targeted sequencing in 348 tumor specimens obtained prior to treatment with CDK4/6i demonstrated that loss-of-function mutations in the *FAT1* tumor suppressor resulted in resistance to CDK4/6i. Interestingly, *FAT1* was shown to result in upregulation of CDK6 expression via the Hippo pathway *in vitro* (36). Finally, recent work from our institution demonstrated that miRNAs modulate CDK6 expression via the TGF β pathway to alter sensitivity to CDK4/6i *in vitro* (37). Increased expression of the implicated miRNA (miR-432-5p) correlated with resistance in a subset of the patients with breast cancer exposed to CDK4/6i from the cohort analyzed here (37). In our study, we did not find examples of activating events in CDK6, nor did we identify *FAT1* alterations among resistant samples. Deletion and truncation mutations in *FAT1* appear to be extremely rare (reported in 6 of 348 patients in Li and colleagues; ref. 36). Given their very low frequency and our sample size ($n = 58$ patients), our study was likely not sufficiently powered to identify this rare event.

CCND1 alterations were modestly enriched among resistant biopsies in our study; however, no association between *CCND1* and tumor response to CDK4/6i was present in tumor specimens from both the randomized PALOMA-1 and PALOMA-3 studies (21, 38). More recent correlative analyses from PALOMA-3 suggested that *CCNE1* expression is associated with inferior outcome for patients receiving palbociclib (21). Although we did not see examples of *CCNE1* amplification in this cohort, we do provide, to our knowledge, the first evidence that *CCNE2* amplification is also associated with the resistant phenotype. Of note, given its proximity to the centromere, copy-number analysis of *CCNE1* via WES is technically challenging, and this may have resulted in underestimation of amplification events in this gene.

The aurora kinases regulate organization of the mitotic spindle and cell-cycle progression (39). *AURKA* overexpression in breast cancer has been associated with an ER-low/basal phenotype (40). *AURKA* was previously implicated in mediating endocrine resistance via SMAD-dependent downregulation of ER α expression (41). We demonstrate that HR⁺ cells cultured to resistance in CDK4/6i can demonstrate downregulation of RB1 or increased expression of *AURKA*, both of which are associated with increased sensitivity to LY3295668, a novel selective *AURKA* inhibitor. In screens to identify synthetic lethal interactions with an *RB1* mutation in lung cancer and other cancers, the aurora kinases emerged as key targets, and LY3295668 provoked tumor regression in xenograft models of *RB1*-null small-cell lung cancer (33, 42). We provide the first evidence supporting *AURKA* as a mediator of resistance to CDK4/6i *in vitro* and in tumor samples. Furthermore, in a patient with HR⁺ MBC

who progressed after a prolonged course of CDK4/6i-based therapy (analogous to our translational culture-to-resistance experiment *in vitro*), subsequent treatment on a phase I trial with LY3295668 was well tolerated and prompted prolonged clinical benefit. This patient had high RB1 protein expression at the time of therapy initiation, suggesting that her response was not governed by RB1 loss.

Oncogenic Signaling Pathways as Potential Nodes of CDK4/6i Resistance

The data presented here, and elsewhere, have implicated a diverse array of oncogenic signaling pathways in modulating CDK4/6i resistance, both *in vitro* and in patient tumor specimens. In addition to expected alterations in *RB1*, we identified a heterogeneous landscape of resistance, in which a variety of rare activating genomic alterations span a diverse spectrum of potential resistance mediators. We confirm enrichment of activating mutations in *ERBB2* and amplification events in *FGFR2* in resistant patients, and both pathways provoke resistance to antiestrogens and CDK4/6i *in vitro* (22, 23, 32, 35). We present, to our knowledge, the first evidence implicating *AKT1* and *RAS* in mediating resistance to CDK4/6i in patients with breast cancer. Of note, we did not find an association between *PIK3CA* status and CDK4/6i resistance in tumor specimens. *PIK3CA* alterations occurred frequently in both arms of the PALOMA-3 study, again suggesting that they are not necessarily advantageous following CDK4/6i exposure (14). *PTEN* alterations were identified in tumor specimens obtained in the setting of ribociclib resistance, and *PTEN* modulation provoked CDK4/6i resistance *in vitro*, perhaps via *AKT1* activation (17).

Targeted sequencing of ctDNA via samples from PALOMA-3 also identified rare events in *ERBB2*, *AKT1*, *KRAS*, and *FGFR2*, which were both acquired and maintained at progression; however, this analysis was limited by lack of insight into the clinical response phenotype of these samples (14). We would hypothesize that “maintained” alterations identified in the context of that study represent instances of early or intrinsic resistance whereas “acquired” alterations are more likely to arise in patients with transient response or clinical benefit from CDK4/6i. *CCNE2* and *AURKA* did not emerge as potential resistance mediators in that study, likely due to lack of insight into copy-number alterations as a result of the sequencing methodology.

Remaining Questions Related to CDK4/6i Resistance

Alterations in *TP53* were enriched in CDK4/6i-resistant biopsies. Mutant *TP53* is not sufficient to promote resistance to CDK4/6i *in vitro*, as MCF7 (*TP53* wild-type) and T47D (*TP53* mutant) are both sensitive at baseline. Knockdown of *TP53* via CRISPR in MCF7 cells did not provoke resistance to palbociclib or abemaciclib *in vitro*. Enrichment of *TP53* mutation in resistant specimens may result from heavier pretreatment (including chemotherapies), may be permissive for the development of other resistance-promoting alterations, or may cooperate with secondary alterations to drive CDK4/6i resistance *in vivo*. Although not sufficient in isolation, the role of *TP53* in CDK4/6i resistance remains an active area of research in the laboratory.

Although all of these mediators provoked resistance *in vitro*, in specific instances there were cell line–dependent differences in their ability to circumvent CDK4/6i. This notion of context specificity is supported by several isolated counterexamples in patients, in which putative resistance mediators were found to occur in individual patients who derived at least transient clinical benefit from CDK4/6i. These findings are also consistent with the spontaneous emergence of distinct resistance mediators in specific cell lines—for example, RAS/ERK-activated and *AURKA*-amplified cells emerged in MDA-MB-361 but not in MCF7, and exogenous overexpression of *AURKA* could not provoke resistance in MCF7. The situation is further complicated by variation in antiestrogen resistance *in vitro*. As an example, *AKT1* overexpression may be sufficient to provoke resistance to both CDK4/6i and fulvestrant, whereas alterations in *RB1* may require a second cooperative event to overcome the antiestrogen component of the regimen (such as *ESR1* alteration). These nuances underscore the complexity of modeling resistance to therapeutic combinations *in vitro* and highlight the need for additional studies to explore context-specific factors, which might dictate the emergence of resistance with a potential driver of interest.

Additional complexity becomes apparent when considering the extent of mutual exclusivity for the various driver alterations (Supplementary Fig. S3). Twelve of 41 resistant biopsy samples (29.3%) had at least two potential resistance drivers. Because bulk exome sequencing was performed, it is not possible to determine where these alterations may be occurring in contemporary subclones or cooperating within the same cells. Additional ongoing work, including single-cell RNA sequencing, may shed new light on these divergent possibilities and provide a deeper understanding of the heterogeneous landscape of resistance.

A minority of samples ($n = 14/41$, 34.1%) lacked any of the eight resistance mediators. Other potential resistance drivers (including *IGF1R*, *MYC*, *NF1*, and others) may contribute to resistance in a subset of samples. Additional preclinical and translational assessment of these resistance mediators is warranted. Alternative, nongenomic, mechanisms of resistance, such as via epigenetic, post-translational, or miRNA-mediated effectors, may also be contributing.

Therapeutic Opportunities for Patients with CDK4/6i Resistance

The majority of alterations identified in our clinical cohort and confirmed *in vitro* are amenable to therapeutic intervention via emerging agents (Fig. 6B). These results suggest that a nonselective regimen is unlikely to yield reliable clinical benefit, whereas a precision-based approach, informed by the underlying genomic findings at progression, could guide selection of therapy in CDK4/6i-resistant patients. RAS-activated cells that emerged under selective pressure with CDK4/6i were highly sensitive to LY3214996, a selective ERK inhibitor. The CHEK1 kinase plays well-established roles in regulating cell-cycle progression in the setting of DNA damage (43). Cancer cells with replication stress caused by activated CDK2 appear to be particularly sensitive to CHEK inhibitors (44), and *CCNE1* amplification has been linked to CHEK1 dependence (34). HR⁺ cells expressing high levels of

CCNE2 demonstrated enhanced sensitivity to prexasertib, a CHEK1 inhibitor that has been well tolerated in human patients, with early evidence suggesting clinical efficacy in a phase I study (45).

CDK4/6i-resistant cells with *RB1* loss or *AURKA* overexpression were sensitive to LY3295668 and, as outlined above, a patient with acquired resistance to palbociclib subsequently derived prolonged clinical benefit from LY3295668 in the context of a phase I clinical trial. Alisertib, an oral *AURKA* inhibitor, was well tolerated in patients with HR⁺ MBC when combined with fulvestrant, and antitumor activity was appreciated in a phase I trial (46). A randomized phase II study of this combination has completed accrual (NCT02860000). Based upon these translational insights, a phase I study exploring the utility of LY3295668 in patients with HR⁺ MBC following progression on CDK4/6i was recently initiated (NCT03955939).

Although one can consider targeting each individual resistance mechanism directly, it may also be possible to target a smaller number of resistance “nodes” or pathways upon which multiple resistance effectors converge. We previously showed that *ERBB2* mutations and alterations in *FGFR1/FGFR2* activate the MAPK pathway in resistant HR⁺ MBC (22, 23), and MAPK pathway inhibition was able to overcome this resistance. *RAS* mutations also activate the MAPK pathway, and several *NF1* alterations were also noted among resistant tumor specimens. The fact that multiple mechanisms of resistance to CDK4/6i activate the MAPK pathway suggests that this may be an important node of resistance in HR⁺ MBC, and that combining endocrine therapy and CDK4/6i with agents that target MAPK such as MEK inhibitors, ERK inhibitors, and/or SHP2 inhibitors, may be a unifying strategy to overcome or prevent resistance resulting from multiple genetic aberrations. Similarly, both *RB* loss and *AURKA* amplification are targetable with *AURKA* inhibitors. Taken together, it may be possible to address all seven of these mechanisms (which account for at least 63% of the resistant biopsies in this study) by targeting four nodes/pathways: *AURKA*, MAPK, *AKT/mTOR*, and *CCNE/CHEK1* (Fig. 6B).

We have identified multiple novel effectors of resistance to CDK4/6i in HR⁺ breast cancer, providing a rationale to guide the development of a wide range of precision-based clinical trials, in which patients with specific genomic or molecular alterations are treated with novel therapeutic combinations designed to circumvent or overcome resistance.

METHODS

Patients and Tumor Samples

Prior to any study procedures, all patients provided written informed consent for research biopsies and WES of tumor and normal DNA, as approved by the Dana-Farber/Harvard Cancer Center IRB (DF/HCC Protocol 05-246). Metastatic core biopsies were obtained from patients, and samples were immediately snap-frozen in OCT and stored in -80°C . Archival formalin-fixed, paraffin-embedded (FFPE) blocks of primary tumor samples were also obtained. A blood sample was obtained during the course of treatment, and whole blood was stored at -80°C until DNA extraction from peripheral blood mononuclear cells (for germline DNA) was performed. In a few instances, cell-free DNA was obtained from plasma for ctDNA analysis, as described previously (47).

Clinical Annotation and Biopsy Phenotypes

Patient charts were reviewed to determine the sequence of treatments received in the neoadjuvant, adjuvant, and metastatic setting as well as the temporal relationship between available biopsy samples and CDK4/6i exposure. Radiographic parameters were assigned via review of the imaging study interpretations available in the patient record during the CDK4/6i treatment course—tumors were defined as “responding” if any degree of tumor shrinkage was reported by the evaluating radiologist, “stable” if there was felt to be no meaningful change, “progressing” if lesions were increasing in size, or “mixed” if comment was made denoting simultaneous shrinkage and growth in discordant lesions. Tumors with a mixed response were excluded from analysis, as a reliable phenotype could not be assigned. The “best radiographic response” (BRR) was then assigned as either “response” (R), “stable disease” (S), or “progression” (P) based upon the best radiographic parameter noted during the CDK4/6i treatment course.

Sensitive biopsies were defined as baseline samples obtained within 120 days prior to, or up to a maximum of 31 days after, CDK4/6i treatment initiation in a patient with subsequent clinical benefit (radiographic response or stable disease >6 months). Biopsies reflecting acquired resistance were obtained from patients who had experienced clinical benefit with CDK4/6i and had an available biopsy specimen either within 31 days of progression or at any time thereafter. Biopsies reflecting intrinsic resistance were obtained within 120 days prior to CDK4/6i initiation in patients without evidence of clinical benefit (defined as progression on the first interval restaging study or stable disease <6 months).

WES

DNA was extracted from primary tumors, metastatic tumors, and peripheral blood mononuclear cells (for germline DNA) from all patients, and WES was performed as detailed below. In several instances, cell-free DNA was obtained from plasma for circulating tumor DNA analysis, as described previously (47).

DNA Extraction. DNA extraction was performed as described previously (48). For whole blood, DNA was extracted using magnetic bead-based chemistry in conjunction with the Chemagic MSM I instrument manufactured by Perkin Elmer. Following red blood cell lysis, magnetic beads bound to the DNA and were removed from solution using electromagnetized rods. Several wash steps followed to eliminate cell debris and protein residue from DNA bound to the magnetic beads. DNA was then eluted in TE buffer. For frozen tumor tissue, DNA and RNA were extracted simultaneously from a single frozen tissue or cell pellet sample using the AllPrep DNA/RNA Kit (Qiagen). For FFPE tumor tissues, DNA and RNA were extracted simultaneously using Qiagen’s AllPrep DNA/RNA FFPE Kit. All DNA is quantified using PicoGreen.

Library Construction. DNA libraries for massively parallel sequencing were generated as described previously (48) with the following modifications: The initial genomic DNA input into the shearing step was reduced from 3 µg to 10–100 ng in 50 µL of solution. For adapter ligation, Illumina paired-end adapters were replaced with palindromic forked adapters (purchased from Integrated DNA Technologies) with unique dual indexed 8 base index molecular barcode sequences included in the adapter sequence to facilitate downstream pooling. With the exception of the palindromic forked adapters, all reagents used for end repair, A-base addition, adapter ligation, and library enrichment PCR were purchased from KAPA Biosciences in 96-reaction kits. In addition, during the postenrichment solid-phase reversible immobilization (SPRI) bead cleanup, elution volume was reduced to 30 µL to maximize library concentration, and a vortexing step was added to maximize the amount of template eluted.

Solution-Phase Hybrid Selection. After library construction, hybridization and capture were performed using the relevant components of Illumina’s Rapid Capture Exome Kit following the manufacturer’s suggested protocol, with the following exceptions: First, all libraries within a library construction plate were pooled prior to hybridization. Second, the Midi plate from Illumina’s Rapid Capture Exome Kit was replaced with a skirted PCR plate to facilitate automation. All hybridization and capture steps were automated on the Agilent Bravo liquid handling system.

Preparation of Libraries for Cluster Amplification and Sequencing. After postcapture enrichment, library pools were then quantified using quantitative PCR (KAPA Biosystems) with probes specific to the ends of the adapters; this assay was automated using Agilent’s Bravo liquid handling platform. On the basis of qPCR quantification, libraries were normalized and denatured using 0.1 N NaOH on the Hamilton Starlet.

Cluster Amplification and Sequencing. Cluster amplification of denatured templates was performed according to the manufacturer’s protocol (Illumina) using HiSeq 2500 Rapid Run v1/v2, HiSeq 2500 High Output v4, or HiSeq 4000 v1 cluster chemistry, and HiSeq 2500 (Rapid or High Output) or HiSeq 4000 flowcells. Flowcells were sequenced on HiSeq 2500 using v1 (Rapid Run flowcells) or v4 (High Output flowcells) Sequencing-by-Synthesis chemistry or v1 Sequencing-by-Synthesis chemistry for HiSeq 4000 flowcells. The flowcells were then analyzed using RTA v.1.18.64 or later. Each pool of whole-exome libraries was run on paired 76 bp runs, with a two 8 base index sequencing reads to identify molecular indices, across the number of lanes needed to meet coverage for all libraries in the pool.

Sequence Data Processing. Exome sequence data processing was performed using established analytic pipelines at the Broad Institute. A BAM file was produced with the Picard pipeline (see URLs) which aligns the tumor and normal sequences to the hg19 human genome build using Illumina sequencing reads. The BAM was uploaded into the Firehose pipeline (see URLs), which manages input and output files to be executed by GenePattern (49).

Sequencing Quality Control. Quality-control modules within Firehose were applied to all sequencing data for comparison of the origin for tumor and normal genotypes and to assess fingerprinting concordance. Cross-contamination of samples was estimated using ContEst (50).

Somatic Alteration Assessment

MuTect (51) was applied to identify somatic single-nucleotide variants. Indelocator (see URLs), Strelka (52), and MuTect2 (see URLs) were applied to identify small insertions or deletions (indels). A voting scheme with at least 2 calls out of 3 algorithms was used to infer indels.

Artifacts introduced by DNA oxidation (so-called OxoG) during sequencing were computationally removed using a filter-based method (53). In the analysis of primary tumors that are FFPE samples, we further applied a filter to remove FFPE-related artifacts (54).

Reads around mutated sites were realigned with Novoalign (see URLs) to filter out false positives that are due to regions of low reliability in the reads alignment. At the last step, we filtered mutations that are present in a comprehensive WES panel of 8,334 normal samples (using the Agilent technology for WES capture) aiming to filter either germline sites or recurrent artifactual sites. We further used a smaller WES panel of 355 normal samples that were based on Illumina technology for WES capture, and another panel of 140 normals sequenced within our cohort (24) to further capture possible batch-specific artifacts. Annotation of identified variants was done using Oncotator (55).

Copy-Number and Copy-Ratio Analysis

To infer somatic copy number from WES, we used ReCapSeg (see URLs), calculating proportional coverage for each target region (i.e., reads in the target/total reads) followed by segment normalization using the median coverage in a panel of normal samples. The resulting copy ratios were segmented using the circular binary segmentation algorithm (56).

To infer allele-specific copy ratios, we mapped all germline heterozygous sites in the germline normal sample using GATK Haplotype Caller (57) and then evaluated the read counts at the germline heterozygous sites to assess the copy profile of each homologous chromosome. The allele-specific copy profiles were segmented to produce allele-specific copy ratios.

Gene Deletions and Biallelic Inactivation

For the inference of gene deletions and inactivations, as we aimed to infer biallelic inactivations (BiDel or “HOMDEL”), we took into account various mutational events that may result in inactivation of both alleles. These mutational events include: (i) loss of heterozygosity (LOH), (ii) single-nucleotide variant (SNV; while excluding the following variant classifications: “Silent,” “Intron,” “IGR,” “5’UTR,” “3’UTR,” “5’Flank,” “3’Flank”), (iii) short indels, (iv) long deletions and gene rearrangements inferred by SvABA (58), and (v) potentially pathogenic germline events in cancer genes (see description below).

Potentially pathogenic germline events: Aiming to retain a subset of potentially pathogenic germline events, there are several features that are accounted for, including (i) ClinVar significant annotation among the following: Pathogenic, Likely pathogenic, Conflicting interpretations of pathogenicity, risk factor or (ii) Variant Classification among the following: Splice_Site, Frame_Shift_Del, Frame_Shift_Ins, Nonsense_Mutation, and (iii) Genome Aggregation Database (gnomAD; ref. 59) less than 0.05 (indicating it is a rare variant).

Cancer Cell Fraction and Evolutionary Analysis

Analysis Using ABSOLUTE. To properly compare SNVs and indels in paired metastatic and primary samples, we considered the union of all mutations called in either of the two samples. We evaluated the reference and alternate reads in each patient’s primary and metastatic tumors, including mutations that were not initially called in one of the samples. These mutations in matched samples were used as input for ABSOLUTE (60). The ABSOLUTE algorithm uses mutation-specific variant allele fractions (VAF) together with the computed purity, ploidy, and segment-specific allelic copy ratio to compute cancer cell fractions (CCF).

Clonal Structure and Phylogenetic Reconstruction of Tumor Evolution. The clonal structure observed in individuals with more than a single tumor sample was inferred with PyClone (61), using the Beta Binomial model and the copy number of each mutation inferred by ABSOLUTE with the parental copy number parameter. Subsequently, the inferred clonal structure was used to trace the evolutionary history of the clones (phylogenetic tree) using the ClonEvol (62), retaining only clones with at least four mutations and estimated cancer cellular fraction (cellular prevalence) higher than 1%. In a single patient (0300397), an *ERBB2*^{L869R} alteration was identified in the acquired resistant biopsy; when an archival pretreatment specimen was analyzed, the *ERBB2*^{L869R} alteration was in low representation (<1% of the cancer cells fraction), but present in a higher fraction using a concurrent targeted sequencing assay applied for this tumor. Conservatively, we defined the *ERBB2*^{L869R} alteration as truncal for the purposes of the phylogenetic evolutionary analysis (Fig. 2G).

Evolutionary Analysis of Copy-Number Variation

Corrected Quantification of Copy Number. Gene amplifications are based on the purity corrected measure for the segment containing that gene, based on ABSOLUTE (rescaled_total_cn; ref. 60). To

better measure segment-specific copy number, we subtracted the genome ploidy for each sample to compute copy number above ploidy (CNAP). CNAPs of at least 3 are considered as amplifications (“AMP”); CNAPs above 1.5, but below 3 are considered low amplification (“GAIN”) and are not depicted in our mutational landscape (Fig. 1). CNAPs of at least 6 are considered high amplifications (“HighAMP”), and CNAPs of at least 9 and no more than 100 genes (63) are considered very high focal amplification (“FocalAMP”).

The evolutionary classification of amplifications accounts for the magnitude of the observed copy-number difference between the pretreatment and the post-treatment samples. If the difference between the CNAP of the post-treatment and the CNAP of the pretreatment is smaller than 50%, the amplification is defined as “Shared.” If the CNAP of the post-treatment is larger than the CNAP by more than 50% and the lower pretreatment CNAP is not at “FocalAMP” level, the evolutionary classification is “Acquired.” If CNAP of the post-treatment is smaller by at least 50% comparing with the pretreatment sample and the lower post-treatment CNAP is not at “FocalAMP” level, the evolutionary classification is “Loss.” Otherwise, the evolutionary classification of amplifications is defined as “Indeterminate.”

Cell Culture

HR⁺/HER2⁻ human breast cancer cell lines T47D (HT-133) and MCF7 (HTB-22) were obtained from ATCC. T47D and MCF7 cells were cultured in RPMI1640 medium (no phenol red; Gibco, 11835-030) and MEMα (nucleosides, no phenol red; Gibco, 41061029) respectively, both supplemented with 10% FBS (Gemini bio-products, 100-106) and 1% penicillin-streptomycin-glutamine. *HEK 293T/17* cells (CRL-11268) were obtained from ATCC and cultured in DMEM (high glucose, pyruvate; Gibco, 11995065), supplemented with 10% FBS (Gemini bioproducts, 100-106) and 1% penicillin-streptomycin-glutamine (Gibco, 10378016).

Candidate Driver Plasmid and Cell Line Production

AKT1 (BRDN0000464992), *KRAS*^{G12D} (BRDN0000553331), *AURKA* (TRCN0000492002), *CCNE2* (ccsbBroadEn_11340), and GFP bacterial streaks were obtained from the Genetic Perturbation Platform, Broad Institute. *RBI* and CRISPR nontargeting guide cells were a gift from Flora Luo and the Garraway laboratory at Emory University. The *CCNE2* construct was cloned into a pLX307 vector using the LR Reaction Kit (Life Technologies, 11791019). All construct plasmids were prepared using the Plasmid Plus Midi Kit (Qiagen, 12943). To generate lentivirus for each construct, 293T cells were transfected with Opti-MEM (Gibco, 31985-062), FuGENE HD (Promega, E2311), VSV-G envelope plasmid, and 8.91 packaging plasmid. After 72-hour incubation, supernatant was filtered through a 0.45 μL filter (Corning, 431225) and lentivirus presence was tested using Lenti-X GoStix (TakaraBio, 631244). 500 μL to 1 mL of virus was added to a 60-mm dish containing T47D (or MCF7) cells and medium with 4 μg/mL of polybrene (Millipore Sigma, TR-1003-G). After overnight incubation, cells were moved to a 100-mm dish and again incubated overnight. The medium was replaced and 0.5 μg/mL of puromycin (Gibco, A1113803) was added to *KRAS*^{G12D}, *AURKA*, *CCNE2*, *RBI*, and CRISPR constructs, and 6–10 μg/mL of blasticidin (Gibco, A1113903) was added to GFP and *AKT1* constructs. Plates were compared with uninfected control plates, and after 2 days of selection, were plated for drug sensitivity assay and harvested for Western blotting as described below.

For the *TP53* knockdown studies, plasmid for CRISPR was constructed by inserting oligonucleotides (sgRNA: CAGAATGCCAAGAGCCAGAG) targeting *TP53* into the lentiCRISPR-v2 vector (BioVector, catalog no. 52961). Electroporation was performed to transfect the plasmid into MCF7 cells. Twenty-four hours after transfection, cells were selected with puromycin (Invitrogen, catalog

no. A1113803) for an additional 3 days. Single knockout clones were then isolated, screened by Western blot with p53 antibody (see below, Cell Signaling Technology, catalog no. 2524), and validated by DNA Sanger sequencing.

Kill Curves/Drug Sensitivity Assay

Cells were plated at a density of 1,000 cells/well in RPMI and 1,500 cells/well in MEM α , for T47D and MCF7, respectively, in 96-well plates (PerkinElmer, 6005181). The experiments were plated in triplicate, for ten doses of the drug of interest. Palbociclib doses ranging from 1 nmol/L to 10 μ mol/L were prepared from a 10 mmol/L stock solution in molecular biology-grade water (Corning, 46-000-CI); abemaciclib doses ranging from 1 nmol/L to 10 μ mol/L were prepared from a 10 mmol/L stock solution in molecular biology-grade water (Corning, 46-000-CI); fulvestrant doses ranging from 0.01 nmol/L to 1 μ mol/L were prepared from a 20 mmol/L stock solution in DMSO (Sigma-Aldrich, D2650). The next day, cells were treated with the range of doses of the drug of interest. Cells were re-treated 3 days later. After treatment was applied for 8 days, the 96-well plates were brought out of the incubator and allowed to equilibrate to room temperature. The medium was replaced with 50 μ L of fresh medium per well. Fifty microliters of CellTiter-Glo 2.0 (Promega, G9241) was added to each well, and the plate was shaken at 200 rpm for 2 minutes and then allowed to equilibrate at room temperature for fifteen minutes as per the CellTiter-Glo 2.0 Assay Technical Manual. Average background luminescence reading was calculated from plate wells containing only medium, and was subtracted from all values. The values were then averaged for each triplicate and SDs were calculated. The data were normalized to the no-drug vehicle control for each construct. The calculated averages and SDs were visualized on GraphPad Prism 7 using the log(inhibitor) versus response (three parameters) preset protocol.

Chemicals and Antibodies

Chemicals utilized included palbociclib (Selleck Chemicals, S1116), abemaciclib (ApexBio, A1794), and fulvestrant (Sigma-Aldrich, I4409). Primary antibodies utilized included antibodies against β -actin (Santa Cruz Biotechnology, sc-47778), RB (Cell Signaling Technology, clone 4H1, 9309, 9307), pRB S780 (Cell Signaling Technology, 3590), pRB S807/811 (Cell Signaling Technology, 8516), AKT (Cell Signaling Technology, 9272), RAS (Cell Signaling Technology, clone D2C1, 8955), Aurora A (Cell Signaling Technology, clone D3E4Q, 14475; R&D Systems AF3295), Cyclin E2 (Cell Signaling Technology, 4132), ERK (Cell Signaling Technology, 3042), pERK T202/Y204 (Cell Signaling Technology, 4370, 4376), BUBR1 (Bethyl Laboratories, A300-386A), MAD2 (BD Transduction Laboratories, 610679), in addition to the secondary antibodies goat anti-rabbit (Invitrogen, 32260) and goat anti-mouse (Invitrogen, A16090).

Western Blotting

A near-confluent T75 ($\sim 7 \times 10^6$ cells) was spun down and the pellet kept at -20°C . The pellet was then lysed in 1 mL of lysis buffer consisting of RIPA buffer (Sigma-Aldrich, R0278), dithiothreitol (DTT; Invitrogen, 15508013), phenylmethane sulfonyl fluoride (PMSF; Sigma-Aldrich, P7626), and PhosStop (Sigma-Aldrich, 4906837001). Lysate was rotated at 15 r.p.m. for 15 minutes at 4°C , and then centrifuged at $14,000 \times g$ for 15 minutes at 4°C , preserving the supernatant. Protein concentration was quantified via bicinchoninic acid (BCA) assay (Pierce BCA Protein Assay Kit, Thermo Fisher Scientific, 23225) and Tecan i-control software preset BCA program. Samples were prepared using 40 μ g of protein, Bolt LDS Sample Buffer (Invitrogen, B0007), and DTT and heated to 95°C for 5 minutes. The samples were run on a Bolt 4%–12% Bis-Tris Plus Gel (Invitrogen, NW04120BOX) in 1 \times Bolt MOPS SDS Running Buffer (Invitrogen,

B000102) for 1 hour at 130 V. Protein was transferred to nitrocellulose membranes via the Trans-Blot Turbo Transfer System (Bio-Rad, 1704150) following the turbo mini preset protocol (1.3A 25V 7Min) two times. Membranes were blocked in 5% milk in Tris-buffered saline (Bio-Rad, 1706435) with 0.1% Tween-20 (Sigma-Aldrich, P9416) for 1 hour at room temperature. Membranes were incubated overnight at 4°C with primary antibodies that were diluted 1:1,000 (with the exception of RB, which was diluted 1:500) in 5% milk in TBS-T. After incubation, membranes were washed three times for 10 minutes with 1 \times TBS-T and incubated with secondary antibody diluted 1:2,000 in 5% milk in TBS-T for 1 hour at room temperature. Membranes were then washed three times for 10 minutes with 1 \times TBS-T. After washing, membranes were treated with Pierce ECL Plus Western Blotting Substrate (Thermo Fisher Scientific, 32132) for 5 minutes and exposed to autoradiography film (Denville, 1159M38).

For resistant/derivative cell lines, cells were washed with PBS and lysed in lysis buffer (1% Triton X-100, 25 mmol/L Tris pH 7.5, 150 mmol/L NaCl, 1 mmol/L EDTA, Halt Protease/phosphatase inhibitor cocktail), and protein concentration was assessed by BCA protein assay (Pierce 23225). Equal amounts of protein were electrophoresed on 4%–20% Bio-Rad Tris Glycine Gels (Bio-Rad 5671094) transferred to nitrocellulose (Bio-Rad 1704159) and probed with primary antibodies. Digiwest protein profiling of MDA-MB-361-AR was also conducted with NMI TT.

Resistant Cell Line Generation

The methods for generating resistant cell lines were described previously (33). Briefly, MDA-MB-361, T47D, and MCF-7 ER⁺ breast cancer cell lines were used to derive variants with acquired resistance to abemaciclib or palbociclib. T47D (HTB-133), MCF-7 (HTB-22), and MDA-MB-361 (HTB-27) were purchased from ATCC. Cell lines were cultured in RPMI1640 medium (Gibco 22400-089) + 10% FBS (Hyclone SH30071.03), Eagle Essential Medium (Gibco 11090-081) + 10% FBS and Liebovitz L-15 Medium (Gibco 11215-064) + 20% FBS, respectively. Resistant cell lines were generated by chronic treatment with either abemaciclib or palbociclib alone or in combination with fulvestrant. Cell cultures were initiated in low doses of compound approximating IC₅₀ until cells grew to 80% confluence. Cells were then passaged and treated with incrementally higher doses. This process was repeated several times until cells were able to grow in the presence of drugs at clinically meaningful concentrations. Once resistant cell lines were established, the stability of resistance was assessed with a 21-day dosing holiday. Resistance remained stable in all cell lines except for T47D-AR and T47D-PR, which became almost completely resensitized to the CDK4/6i after the 21-day drug-free period. All resistant derivatives were found to be cross-resistant to the CDK4/6i that was not used in the selection step. Short tandem repeat (STR) analysis was performed to verify the authenticity of the cell lines.

Proliferation Assays

Cells were plated onto poly-D-lysine plates (Corning 354640) and treated in replicate with a dose curve of compounds of interest. Cells were allowed to grow for two doubling times, and proliferation was measured by CellTiter-Glo (Promega G7571) or CyQuant (Invitrogen C3511) as per the manufacturer's protocol. Data analysis was carried out using Prism software.

Apoptosis Assay

MCF7 and MCF7-PR-1 cells were treated with increasing doses of prexasertib for 48 and 72 hours. DMSO treatment was utilized as a negative control. For a positive control, cells were treated with STSP (4 μ mol/L) for 4 hours. Cells were subsequently stained with Annexin V-FITC Apoptosis Detection Kit (Sigma, APOAF). Apoptotic cell percentage was counted with FACS.

LY3295668 Phase I/II Clinical Trial

The patient vignette provided in this article was shared from an ongoing phase I/II study. Please see protocol NCT03092934 at www.clinicaltrials.gov for details related to the study location, eligibility, and compound. This is an open-label, multicenter study of patients with locally advanced or metastatic solid tumors and disease progression after 1 to 4 prior treatment regimens. The phase I portion of the protocol is designed to evaluate the primary objective of determining the MTD; secondary objectives included evaluation of tolerability and overall safety profile of LY3295668. The primary objective of the phase II study portion is to evaluate the objective response rate of tumors after treatment with LY3295668. Patients in the phase II study were required to have estrogen receptor- and/or progesterone receptor-positive, HER2-negative breast cancer with prior exposure to and progression on a hormone therapy and a CDK4/6 inhibitor.

URLs

Picard, <https://sourceforge.net/projects/picard/>; Firehose, <http://www.broadinstitute.org/cancer/cga/Firehose>; Indelocator, <http://www.broadinstitute.org/cancer/cga/indelocator>; MuTect2, https://software.broadinstitute.org/gatk/documentation/tooldocs/current/org_broadinstitute_gatk_tools_walkers_cancer_m2_MuTect2; Novoalign, www.novocraft.com/products/novoalign/; ReCapSeg, <http://gatkforums.broadinstitute.org/categories/recapseg-documentation>

Disclosure of Potential Conflicts of Interest

S.A. Wander is a consultant at Foundation Medicine, InfiniteMD, Eli Lilly, and Puma Biotechnology, and reports receiving commercial research support from Genentech. X. Gong is a researcher at Eli Lilly and Company, and has ownership interest (including patents) in Eli Lilly and Company. L.M. Litchfield is an employee at Eli Lilly and Company, and has ownership interest (including patents) in Eli Lilly and Company. V.M. Jansen is a senior medical advisor at and has ownership interest (including patents) in Eli Lilly and Company. G.J. Oakley is a senior medical advisor at Eli Lilly and Company. J.D. Kremer is a clinical research physician at Eli Lilly and medical director at Taiho Oncology Inc. E.P. Winer is a consultant at Carrick Therapeutics, G1 Therapeutics, Syros, Genentech, Genomic Health, GSK, Jounce, Leap, Lilly, Novartis, and Seattle Genetics. S.M. Tolane is a consultant at AstraZeneca, Eli Lilly, Puma, Sanofi, Odonate, Seattle Genetics, Silverback Therapeutics, G1 Therapeutics, AbbVie, Anthenex, OncoPep, Merck, Nektar, Novartis, Pfizer, Genentech, Immunomedics, Bristol-Myers Squibb, and NanoString, and reports receiving commercial research grants from Merck (all funding to institute), Novartis (all funding to institute), Pfizer (all funding to institute), and Eli Lilly (all funding to institute). N.U. Lin reports receiving commercial research grants from Genentech, Seattle Genetics, Pfizer, and Merck, and is a consultant/advisory board member for Puma, Seattle Genetics, and Daichii Sankyo. S.G. Buchanan is a senior research fellow at Eli Lilly, and has ownership interest (including patents) in Eli Lilly. N. Wagle is a consultant/advisory board member at Eli Lilly, Novartis, and Relay Therapeutics, reports receiving a commercial research grant from Puma Biotechnology (all funding to institute), and has ownership interest (including patents) in Relay Therapeutics. No potential conflicts of interest were disclosed by the other authors.

Authors' Contributions

Conception and design: S.A. Wander, O. Cohen, X. Gong, F. Luo, K.J. Kowalski, X.S. Ye, L.A. Garraway, E.P. Winer, N.U. Lin, S.G. Buchanan, N. Wagle

Development of methodology: S.A. Wander, O. Cohen, P. Mao, U. Nayyar, S.H. Parsons, X.S. Ye, C. Yu, P.S. Smith, L.A. Garraway, N. Wagle

Acquisition of data (provided animals, acquired and managed patients, provided facilities, etc.): S.A. Wander, G.N. Johnson, M.R. Lloyd, K.J. Kowalski, A.G. Waks, R. Martinez, L.M. Litchfield, X.S. Ye, C. Yu, V.M. Jansen, J.R. Stille, P.S. Smith, G.J. Oakley, M.E. Hughes, J.D. Kremer, N.U. Lin, N. Wagle

Analysis and interpretation of data (e.g., statistical analysis, biostatistics, computational analysis): S.A. Wander, O. Cohen, X. Gong, G.N. Johnson, J.E. Buendia-Buendia, M.R. Lloyd, D. Kim, K.J. Kowalski, S.H. Parsons, R. Martinez, J.R. Stille, P.S. Smith, G.J. Oakley, G. Batist, S.G. Buchanan, N. Wagle

Writing, review, and/or revision of the manuscript: S.A. Wander, O. Cohen, G.N. Johnson, P. Mao, A.G. Waks, X.S. Ye, V.M. Jansen, J.R. Stille, G.J. Oakley, Q.S. Chu, G. Batist, J.D. Kremer, E.P. Winer, N.U. Lin, S.G. Buchanan, N. Wagle

Administrative, technical, or material support (i.e., reporting or organizing data, constructing databases): M.R. Lloyd, D. Kim, F. Luo, M.E. Hughes, N.U. Lin, N. Wagle

Study supervision: X. Gong, K. Helvie, X.S. Ye, J.R. Stille, P.S. Smith, N.U. Lin, S.G. Buchanan, N. Wagle

Acknowledgments

We thank Laura Dellostritto, Lori Marini, Nelly Oliver, Shreevidya Periyasamy, Janet Files, Sara Hoffman, and Colin Mackichan for assistance with patient sample collection and annotation. We are grateful to all the patients who volunteered for our tumor biopsy protocol and generously provided the tissue analyzed in this study. This work was supported by the Department of Defense W81XWH-13-1-0032 (to N. Wagle), Landon Foundation-AACR INNOVATOR Award for Research in Personalized Cancer Medicine, 13-60-27-WAGL (to N. Wagle), NCI Breast Cancer SPORE at DF/HCC #P50CA168504 (to N. Wagle, N.U. Lin, and E.P. Winer), Susan G. Komen CCR1533343 (to N. Wagle), The V Foundation (to N. Wagle), The Breast Cancer Alliance (to N. Wagle), The Cancer Couch Foundation (to N. Wagle), Twisted Pink (to N. Wagle), Hope Scarves (to N. Wagle), Breast Cancer Research Foundation (to N.U. Lin and E.P. Winer), ACT NOW (to Dana-Farber Cancer Institute Breast Oncology Program), Fashion Footwear Association of New York (to Dana-Farber Cancer Institute Breast Oncology Program), Friends of Dana-Farber Cancer Institute (to N. U. Lin), National Comprehensive Cancer Network/Pfizer Independent Grant for Learning & Change (to N.U. Lin), the Dana-Farber Cancer Institute T32 (to S.A. Wander), Wong Family Translational Research Award (to S.A. Wander), and the Conquer Cancer Foundation/Twisted Pink/American Society of Clinical Oncology Young Investigator Award (to S.A. Wander).

The costs of publication of this article were defrayed in part by the payment of page charges. This article must therefore be hereby marked *advertisement* in accordance with 18 U.S.C. Section 1734 solely to indicate this fact.

Received November 27, 2019; revised March 29, 2020; accepted May 8, 2020; published first May 13, 2020.

REFERENCES

- Spring LM, Wander SA, Zangardi M, Bardia A. CDK 4/6 inhibitors in breast cancer: current controversies and future directions. *Curr Oncol Rep* 2019;21:25.
- Ballinger TJ, Meier JB, Jansen VM. Current landscape of targeted therapies for hormone-receptor positive, her2 negative metastatic breast cancer. *Front Oncol* 2018;8:308.
- Finn RS, Martin M, Rugo HS, Jones S, Im SA, Gelmon K, et al. Palbociclib and letrozole in advanced breast cancer. *N Engl J Med* 2016;375:1925–36.
- Cristofanilli M, Turner NC, Bondarenko I, Ro J, Im SA, Masuda N, et al. Fulvestrant plus palbociclib versus fulvestrant plus placebo

- for treatment of hormone-receptor-positive, HER2-negative metastatic breast cancer that progressed on previous endocrine therapy (PALOMA-3): final analysis of the multicentre, double-blind, phase 3 randomised controlled trial. *Lancet Oncol* 2016;17:425–39.
5. Hortobagyi GN, Stemmer SM, Burris HA, Yap YS, Sonke GS, Paluch-Shimon S, et al. Ribociclib as first-line therapy for HR-positive, advanced breast cancer. *N Engl J Med* 2016;375:1738–48.
 6. Goetz MP, Toi M, Campone M, Sohn J, Paluch-Shimon S, Huober J, et al. MONARCH 3: abemaciclib as initial therapy for advanced breast cancer. *J Clin Oncol* 2017;35:3638–46.
 7. Sledge GW Jr, Toi M, Neven P, Sohn J, Inoue K, Pivot X, et al. MONARCH 2: abemaciclib in combination with fulvestrant in women with HR+/HER2– advanced breast cancer who had progressed while receiving endocrine therapy. *J Clin Oncol* 2017;35:2875–84.
 8. Sledge GW Jr, Toi M, Neven P, Sohn J, Inoue K, Pivot X, et al. The effect of abemaciclib plus fulvestrant on overall survival in hormone receptor-positive, ERBB2-negative breast cancer that progressed on endocrine therapy-MONARCH 2: a randomized clinical trial. *JAMA Oncol* 2020;6:116–24.
 9. Im SA, Lu YS, Bardia A, Harbeck N, Colleoni M, Franke F, et al. Overall survival with ribociclib plus endocrine therapy in breast cancer. *N Engl J Med* 2019;381:307–16.
 10. Dickler MN, Tolane SM, Rugo HS, Cortés J, Diéras V, Patt D, et al. MONARCH 1, A phase II study of abemaciclib, a CDK4 and CDK6 inhibitor, as a single agent, in patients with refractory HR(+)/HER2(–) metastatic breast cancer. *Clin Cancer Res* 2017;23:5218–24.
 11. Finn RS, Dering J, Conklin D, Kalous O, Cohen DJ, Desai AJ, et al. PD 0332991, a selective cyclin D kinase 4/6 inhibitor, preferentially inhibits proliferation of luminal estrogen receptor-positive human breast cancer cell lines in vitro. *Breast Cancer Res* 2009;11:R77.
 12. Herrera-Abreu MT, Palafox M, Asghar U, Rivas MA, Cutts RJ, Garcia-Murillas I, et al. Early adaptation and acquired resistance to CDK4/6 inhibition in estrogen receptor-positive breast cancer. *Cancer Res* 2016;76:2301–13.
 13. Condorelli R, Spring L, O’Shaughnessy J, Lacroix L, Bailleux C, Scott V, et al. Polyclonal RB1 mutations and acquired resistance to CDK 4/6 inhibitors in patients with metastatic breast cancer. *Ann Oncol* 2018;29:640–5.
 14. O’Leary B, Cutts RJ, Liu Y, Hrebien S, Huang X, Fenwick K, et al. The genetic landscape and clonal evolution of breast cancer resistance to palbociclib plus fulvestrant in the PALOMA-3 Trial. *Cancer Discov* 2018;8:1390–403.
 15. Friebens C, O’Leary B, Kilburn L, Hrebien S, Garcia-Murillas I, Beaney M, et al. Plasma ESR1 mutations and the treatment of estrogen receptor-positive advanced breast cancer. *J Clin Oncol* 2016;34:2961–8.
 16. Tolane SM, Toi M, Neven P, Sohn J, Grischke E-M, Llombart-Cussac A, et al. Abstract 4458: Clinical significance of *PIK3CA* and *ESR1* mutations in ctDNA and FFPE samples from the MONARCH 2 study of abemaciclib plus fulvestrant. *Cancer Res* 2019;79:4458.
 17. Costa C, Wang Y, Ly A, Hosono Y, Murchie E, Walmsley CS, et al. PTEN loss mediates clinical cross-resistance to CDK4/6 and PI3K/alpha inhibitors in breast cancer. *Cancer Discov* 2020;10:72–85.
 18. Jansen VM, Bholra NE, Bauer JA, Formisano L, Lee KM, Hutchinson KE, et al. Kinome-wide RNA interference screen reveals a role for PDK1 in acquired resistance to CDK4/6 inhibition in ER-positive breast cancer. *Cancer Res* 2017;77:2488–99.
 19. Yang C, Li Z, Bhatt T, Dickler M, Giri D, Scaltriti M, et al. Acquired CDK6 amplification promotes breast cancer resistance to CDK4/6 inhibitors and loss of ER signaling and dependence. *Oncogene* 2017;36:2255–64.
 20. Caldon CE, Sergio CM, Kang J, Muthukaruppan A, Boersma MN, Stone A, et al. Cyclin E2 overexpression is associated with endocrine resistance but not insensitivity to CDK2 inhibition in human breast cancer cells. *Mol Cancer Ther* 2012;11:1488–99.
 21. Turner NC, Liu Y, Zhu Z, Loi S, Colleoni M, Loibl S, et al. Cyclin E1 expression and palbociclib efficacy in previously treated hormone receptor-positive metastatic breast cancer. *J Clin Oncol* 2019;37:169–78.
 22. Mao P, Cohen O, Kowalski K, Kusiel J, Buendia J, Exman P, et al. Acquired FGFR and FGF alterations confer resistance to estrogen receptor (ER) targeted therapy in ER+ metastatic breast cancer. *bioRxiv* 2019:605436.
 23. Nayar U, Cohen O, Kapstad C, Cuoco MS, Waks AG, Wander SA, et al. Acquired HER2 mutations in ER(+) metastatic breast cancer confer resistance to estrogen receptor-directed therapies. *Nat Genet* 2019;51:207–16.
 24. Cohen O, Kim D, Oh C, Waks A, Oliver N, Helvie K, et al. Whole exome and transcriptome sequencing of resistant ER+ metastatic breast cancer [abstract]. In: Proceedings of the 2016 San Antonio Breast Cancer Symposium; 2016 Dec 6–10; San Antonio, TX. Philadelphia (PA): AACR; 2017. Abstract nr S1-01.
 25. Abba MC, Gong T, Lu Y, Lee J, Zhong Y, Lacunza E, et al. A molecular portrait of high-grade ductal carcinoma *in situ*. *Cancer Res* 2015;75:3980–90.
 26. Zehir O, Benayed R, Shah RH, Syed A, Middha S, Kim HR, et al. Mutational landscape of metastatic cancer revealed from prospective clinical sequencing of 10,000 patients. *Nat Med* 2017;23:703–13.
 27. Baker R, Wilkerson EM, Sumita K, Isom DG, Sasaki AT, Dohlmans HG, et al. Differences in the regulation of K-Ras and H-Ras isoforms by monoubiquitination. *J Biol Chem* 2013;288:36856–62.
 28. Jeselsohn R, Buchwalter G, De Angelis C, Brown M, Schiff R. ESR1 mutations—a mechanism for acquired endocrine resistance in breast cancer. *Nat Rev Clin Oncol* 2015;12:573–83.
 29. Tate JG, Bamford S, Jubb HC, Sondka Z, Beare DM, Bindal N, et al. COSMIC: the catalogue of somatic mutations in cancer. *Nucleic Acids Res* 2019;47:D941–7.
 30. Marchio C, Geyer FC, Ng CK, Piscuoglio S, De Filippo MR, Cupo M, et al. The genetic landscape of breast carcinomas with neuroendocrine differentiation. *J Pathol* 2017;241:405–19.
 31. Bessiere L, Todeschini AL, Auguste A, Sarnacki S, Flatters D, Legois B, et al. A hot-spot of in-frame duplications activates the oncoprotein AKT1 in juvenile granulosa cell tumors. *EBioMedicine* 2015;2:421–31.
 32. Formisano L, Lu Y, Servetto A, Hanker AB, Jansen VM, Bauer JA, et al. Aberrant FGFR signaling mediates resistance to CDK4/6 inhibitors in ER+ breast cancer. *Nat Commun* 2019;10:1373.
 33. Gong X, Du J, Parsons SH, Merzoug FF, Webster Y, Iversen PW, et al. Aurora a kinase inhibition is synthetic lethal with loss of the RB1 tumor suppressor gene. *Cancer Discov* 2019;9:248–63.
 34. Etemadmoghadam D, Weir BA, Au-Yeung G, Alsop K, Mitchell G, George J, et al.; Australian Ovarian Cancer Study Group. Synthetic lethality between CCNE1 amplification and loss of BRCA1. *Proc Natl Acad Sci U S A* 2013;110:19489–94.
 35. Drago JZ, Formisano L, Juric D, Niemierko A, Servetto A, Wander SA, et al. FGFR1 gene amplification mediates endocrine resistance but retains TORC sensitivity in metastatic hormone receptor positive (HR+) breast cancer. *Clin Cancer Res* 2019;25:6443–51.
 36. Li Z, Razavi P, Li Q, Toy W, Liu B, Ping C, et al. Loss of the FAT1 tumor suppressor promotes resistance to CDK4/6 inhibitors via the hippo pathway. *Cancer Cell* 2018;34:893–905.
 37. Cornell L, Wander SA, Visal T, Wagle N, Shapiro GI. MicroRNA-mediated suppression of the tgf-beta pathway confers transmissible and reversible CDK4/6 inhibitor resistance. *Cell Rep* 2019;26:2667–80.
 38. Finn RS, Crown JP, Lang I, Boer K, Bondarenko IM, Kulyk SO, et al. The cyclin-dependent kinase 4/6 inhibitor palbociclib in combination with letrozole versus letrozole alone as first-line treatment of oestrogen receptor-positive, HER2-negative, advanced breast cancer (PALOMA-1/TRIO-18): a randomised phase 2 study. *Lancet Oncol* 2015;16:25–35.
 39. Willems E, Dedobbeleer M, Digregorio M, Lombard A, Lumapat PN, Rogister B. The functional diversity of Aurora kinases: a comprehensive review. *Cell Div* 2018;13:7.
 40. Staff S, Isola J, Jumppanen M, Tanner M. Aurora-A gene is frequently amplified in basal-like breast cancer. *Oncol Rep* 2010;23:307–12.
 41. Opyrchal M, Salisbury JL, Zhang S, McCubrey J, Hawse J, Goetz MP, et al. Aurora-A mitotic kinase induces endocrine resistance through down-regulation of ERalpha expression in initially ERalpha+ breast cancer cells. *PLoS One* 2014;9:e96995.
 42. Oser MG, Fonseca R, Chakraborty AA, Brough R, Spektor A, Jennings RB, et al. Cells Lacking the RB1 Tumor Suppressor Gene Are

- Hyperdependent on Aurora B Kinase for Survival. *Cancer Discov* 2019;9:230–47.
43. Karnitz LM, Zou L. Molecular pathways: targeting atr in cancer therapy. *Clin Cancer Res* 2015;21:4780–5.
 44. Sakurikar N, Thompson R, Montano R, Eastman A. A subset of cancer cell lines is acutely sensitive to the Chk1 inhibitor MK-8776 as monotherapy due to CDK2 activation in S phase. *Oncotarget* 2016;7:1380–94.
 45. Hong D, Infante J, Janku F, Jones S, Nguyen LM, Burris H, et al. Phase I Study of LY2606368, a checkpoint kinase 1 inhibitor, in patients with advanced cancer. *J Clin Oncol* 2016;34:1764–71.
 46. Haddad TC, D'Assoro A, Suman V, Opyrchal M, Peethambaram P, Liu MC, et al. Phase I trial to evaluate the addition of alisertib to fulvestrant in women with endocrine-resistant, ER+ metastatic breast cancer. *Breast Cancer Res Treat* 2018;168:639–47.
 47. Adalsteinsson VA, Ha G, Freeman SS, Choudhury AD, Stover DG, Parsons HA, et al. Scalable whole-exome sequencing of cell-free DNA reveals high concordance with metastatic tumors. *Nat Commun* 2017;8:1324.
 48. Fisher S, Barry A, Abreu J, Minie B, Nolan J, Delorey TM, et al. A scalable, fully automated process for construction of sequence-ready human exome targeted capture libraries. *Genome Biol* 2011;12:R1.
 49. Reich M, Liefeld T, Gould J, Lerner J, Tamayo P, Mesirov JP. GenePattern 2.0. *Nat Genet* 2006;38:500–1.
 50. Cibulskis K, McKenna A, Fennell T, Banks E, DePristo M, Getz G. ContEst: estimating cross-contamination of human samples in next-generation sequencing data. *Bioinformatics* 2011;27:2601–2.
 51. Cibulskis K, Lawrence MS, Carter SL, Sivachenko A, Jaffe D, Sougnez C, et al. Sensitive detection of somatic point mutations in impure and heterogeneous cancer samples. *Nat Biotechnol* 2013;31:213–9.
 52. Saunders CT, Wong WS, Swamy S, Becq J, Murray LJ, Cheetham RK, Strelka: accurate somatic small-variant calling from sequenced tumor-normal sample pairs. *Bioinformatics* 2012;28:1811–7.
 53. Costello M, Pugh TJ, Fennell TJ, Stewart C, Lichtenstein L, Meldrim JC, et al. Discovery and characterization of artifactual mutations in deep coverage targeted capture sequencing data due to oxidative DNA damage during sample preparation. *Nucleic Acids Res* 2013;41:e67.
 54. Van Allen EM, Wagle N, Stojanov P, Perrin DL, Cibulskis K, Marlow S, et al. Whole-exome sequencing and clinical interpretation of formalin-fixed, paraffin-embedded tumor samples to guide precision cancer medicine. *Nat Med* 2014;20:682–8.
 55. Ramos AH, Lichtenstein L, Gupta M, Lawrence MS, Pugh TJ, Sakseena G, et al. Oncotator: cancer variant annotation tool. *Hum Mutat* 2015;36:E2423–9.
 56. Olshen AB, Venkatraman ES, Lucito R, Wigler M. Circular binary segmentation for the analysis of array-based DNA copy number data. *Biostatistics* 2004;5:557–72.
 57. DePristo MA, Banks E, Poplin R, Garimella KV, Maguire JR, Hartl C, et al. A framework for variation discovery and genotyping using next-generation DNA sequencing data. *Nat Genet* 2011;43:491–8.
 58. Wala JA, Bandopadhyay P, Greenwald NF, O'Rourke R, Sharpe T, Stewart C, et al. SvABA: genome-wide detection of structural variants and indels by local assembly. *Genome Res* 2018;28:581–91.
 59. Walsh R, Thomson KL, Ware JS, Funke BH, Woodley J, McGuire KJ, et al. Reassessment of Mendelian gene pathogenicity using 7,855 cardiomyopathy cases and 60,706 reference samples. *Genet Med* 2017;19:192–203.
 60. Carter SL, Cibulskis K, Helman E, McKenna A, Shen H, Zack T, et al. Absolute quantification of somatic DNA alterations in human cancer. *Nat Biotechnol* 2012;30:413–21.
 61. Roth A, Khattra J, Yap D, Wan A, Laks E, Biele J, et al. PyClone: statistical inference of clonal population structure in cancer. *Nat Methods* 2014;11:396–8.
 62. Dang HX, White BS, Foltz SM, Miller CA, Luo J, Fields RC, et al. ClonEvol: clonal ordering and visualization in cancer sequencing. *Ann Oncol* 2017;28:3076–82.
 63. Ulz P, Belic J, Graf R, Auer M, Lafer I, Fischereder K, et al. Whole-genome plasma sequencing reveals focal amplifications as a driving force in metastatic prostate cancer. *Nat Commun* 2016;7:12008.